 CMC, vol.12, no.2, pp.157-195, 2009

Buckling Analysis of Plates Stiffened by Parallel Beams

E.J. Sapountzakis[1] **and V.G. Mokos**[1]

Abstract: In this paper a general solution for the elastic buckling analysis of plates stiffened by arbitrarily placed parallel beams of arbitrary doubly symmetric cross section subjected to an arbitrary inplane loading is presented. According to the proposed model, the stiffening beams are isolated from the plate by sections in the lower outer surface of the plate, taking into account the arising tractions in all directions at the fictitious interfaces. These tractions are integrated with respect to each half of the interface width resulting two interface lines, along which the loading of the beams as well as the additional loading of the plate is defined. The unknown distribution of the aforementioned integrated tractions is established by applying continuity conditions in all directions at the two interface lines, while the analysis of both the plate and the beams is accomplished on their deformed shape. The method of analysis is based on the capability to establish the elastic and the corresponding geometric stiffness matrices of the stiffened plate with respect to a set of nodal points. Thus, the original eigenvalue problem for the differential equation of buckling is converted into a typical linear eigenvalue problem, from which the buckling loads are established numerically. For the calculation of the elastic and geometric stiffness matrices six boundary value problems are formulated and solved using the Analog Equation Method (AEM), a BEM-based method. Numerical examples with practical interest are presented. The accuracy of the results of the proposed model compared with those obtained from a 3–D FEM solution is remarkable.

Keywords: Stiffened plate, ribbed plate, slab-and-beam structure, buckling, nonuniform torsion, warping, boundary element method.

1 Introduction

Structural plate systems stiffened by beams in one direction are widely used in buildings, bridges, ships, aircrafts and machines resulting an economical, light

[1] School of Civil Engineering, National Technical University, Zografou Campus, GR–157 80, Athens, Greece. Email: cvsapoun@central.ntua.gr, vgmokos@central.ntua.gr

weight design of the structure. While the stiffening elements add negligible weight to the overall structure, their influence on strength and stability is enormous. Stiffened plates can be subjected to high axial forces, high bending moments or combination of both. Due to the presence of the compressive axial forces and bending moments, stiffened panels are susceptible to failure by instability. A reliable and safe design of such plate structures necessitates a rigorous buckling analysis.

The problem of buckling of stiffened plates has been widely studied from both the analytical and the numerical point of view with pioneer the work of Bryan (1891) who applied energy criteria to the study of the stability of plates under uniform compression, while Timoshenko in (1936) and Timoshenko and Gere in (1951) presented numerical tables for buckling loads of rectangular plates stiffened by longitudinal and transverse ribs. The effect of eccentricity of the stiffener was introduced as the effective moment of inertia of the stiffener by Seide (1953), while Troitsky (1976) discussed the earlier developments in this field. However, due to the mathematical complexity of the problem, the existing analytical solutions are limited to stiffened plates of simple geometry, loading and boundary conditions. Thus, numerical methods have been used for the analysis of the aforementioned stability problem. Among these methods the majority of researchers have employed the finite element method (FEM). The first attempt to apply the finite element method to the stability analysis of unstiffened plates is due to Kapur and Hartz (1966) and to stiffened plates is due to Dawe (1969). Later, several finite element solutions (Shastry, Venkateswara, Rao, and Reddy, 1976; Shen , Huang and Wang, 1987; Madhujit and Abhijit, 1990; Meiwen and Issam, 1992; Sabir and Djoudi, 1995; . Grondin, Elwi and Cheng, 1999; Sheikh, Elwi, and Grondin, 2003; Vörös, 2007; Vörös, 2007) have been developed for stability problems of slab-and-beam structures, while the finite strip method has also been used for the aforementioned problem (Lau and Hancock, 1986; Kakol, 1990).

The boundary element method (BEM) (Sapountzakis and Mokos, 2009; Tan et. al., 2009; Liu, 2007; Sapountzakis and Tsiatas, 2007; Dziatkiewicz and Fedelinski, 2007; Wang et. al., 2006; Koziara, and Davies, 2006; Sanz et. al., 2006; Zhou et. al. (2006); Fernandes and Venturini, 2005; Botta and Venturini, 2005; Divo and Kassab, 2005; Shiah et. al., 2005; Sun, et. al., 2004; Mansur et. al, 2004; Miers and Telles, 2004; Rashed, 2004; Zhang and Savaidis, 2003; Hatzigeorgiou and Beskos, 2002; Lie et. al., 2001; Mandolini et. al., 2001; Muller-Karger et. al., 2001; Ochiai, 2001; Providakis, 2000; Shiah, and Tan, 2000; de Paiva, 1996; Katsikadelis and Sapountzakis, 1991; Katsikadelis et. al., 1990; Katsikadelis and Sapountzakis, 1985) on the other hand seems to be an alternative powerful tool for the solution of the aforementioned buckling problem. It is worth here noting that the BEM allows the evaluation of the solution and its derivatives at any point of the plate, using the integral representation of the solution as a continuous mathematical expression, which can be differentiated and utilized as a mathematical formula. In recent years the boundary element method has been successfully applied to the solution of stability problems of unstiffened plate structures. Thus, the boundary element procedure was employed for the buckling analysis of plates with constant (Costa and Brebbia, 1985; Bezine, Cimetiere and Gelbert, 1985; Tanaka, 1986; Manolis, Beskos, and Pineros, 1986; Syngellakis and Kang, 1987; Jauhorng, Roger and Hui-Ru 1999; Purbolaksono and Aliabadi, 2005) or variable thickness (Nerantzaki and Katsikadelis, 1996) and for the post-buckling behavior of plates (Kamiya, Sawaki and Nakamura, 1984; Qinghua and Yuying, 1990; Wen, Aliabadi and Young, 2006; Katsikadelis and Babouskos, 2007). Nevertheless, to the authors' knowledge, the boundary element method has not yet been used for the buckling analysis of stiffened plates.

In this paper a general solution for the elastic buckling analysis of plates stiffened by arbitrarily placed parallel beams of arbitrary doubly symmetric cross section subjected to an arbitrary inplane loading is presented, by improving the employed structural model of Sapountzakis and Mokos (Sapountzakis and Mokos, 2007), so that a nonuniform distribution of the interface transverse shear force and the nonuniform torsional response of the beams are taken into account. According to the improved model, the stiffening beams are isolated from the plate by sections in the lower outer surface of the plate, taking into account the arising tractions in all directions at the fictitious interfaces. These tractions are integrated with respect to each half of the interface width resulting two interface lines, along which the loading of the beams as well as the additional loading of the plate is defined. The utilization of two interface lines for each beam enables the nonuniform torsional response of the beams to be taken into account as the angle of twist is indirectly equated with the corresponding plate slope. The unknown distribution of the aforementioned integrated tractions is established by applying continuity conditions in all directions at the two interface lines, while the analysis of both the plate and the beams is accomplished on their deformed shape. The method of analysis is based on the capability to establish the elastic and the corresponding geometric stiffness matrices of the stiffened plate with respect to a set of nodal points. Thus, the original eigenvalue problem for the differential equation of buckling is converted into a typical linear eigenvalue problem, from which the buckling loads are established numerically. For the calculation of the elastic and geometric stiffness matrices six boundary value problems are formulated and solved using the Analog Equation Method (AEM) (Katsikadelis, 2002), a BEM-based method. Numerical examples with practical interest are presented. The adopted model permits the evaluation of the shear forces at the interfaces in both directions, the knowledge of which is very important in the design of prefabricated ribbed plates. The accuracy of the results of the proposed model compared with those obtained from a 3-D FEM solution (MSC/NASTRAN for Windows, 1999) is remarkable.

2 Statement of the problem

Consider a thin plate of homogeneous, isotropic and linearly elastic material with modulus of elasticity E and Poisson ratio μ, having constant thickness h_p and occupying the two dimensional multiply connected region Ω of the x,y plane bounded by the piecewise smooth $K+1$curves $\Gamma_0, \Gamma_1, ..., \Gamma_{K-1}, \Gamma_K$, as shown in Fig.1. The plate is stiffened by a set of $i = 1, 2, ..., I$ arbitrarily placed parallel beams of arbitrary doubly symmetric cross section and of homogeneous, isotropic and linearly elastic material with modulus of elasticity E_b^i and Poisson ratio μ_b^i, which may have either internal or boundary point supports. For the sake of convenience the x axis is taken parallel to the beams. The stiffened plate is subjected to the lateral load $g = g(x,y)$ and to the inplane external boundary loading N_n^b, N_{nt}^b. For the analysis of the aforementioned problem a global coordinate system Oxy for the analysis of the plate and local coordinate ones $O^i x^i y^i$ corresponding to the centroid axes of each beam are employed as shown in Fig.1.

The solution of the problem at hand is approached by an improved model of that proposed by Sapountzakis and Mokos (2007). According to this model, the stiffening beams are isolated again from the plate by sections in its lower outer surface, taking into account the arising tractions at the fictitious interfaces (Fig.2). Integration of these tractions along each half of the width of the i-th beam results in line forces per unit length in all directions in two interface lines, which are denoted by q_{xj}^i, q_{yj}^i and q_{zj}^i $(j = 1,2)$ encountering in this way the nonuniform distribution of the interface transverse shear forces q_y^i, which in the aforementioned model (Sapountzakis and Mokos, 2007) was ignored. The aforementioned integrated tractions result in the loading of the i-th beam as well as the additional loading of the plate. Their distribution is unknown and can be established by imposing displacement continuity conditions in all directions along the two interface lines, enabling in this way the nonuniform torsional response of the beams to be taken into account, which in the aforementioned model (Sapountzakis and Mokos, 2007) was also ignored.

The arising additional loading at the middle surface of the plate and the loading along the centroid and the shear center axes of each beam can be summarized as follows

a. In the plate (at the traces of the two interface lines j=1,2 of the i-th plate-beam interface)

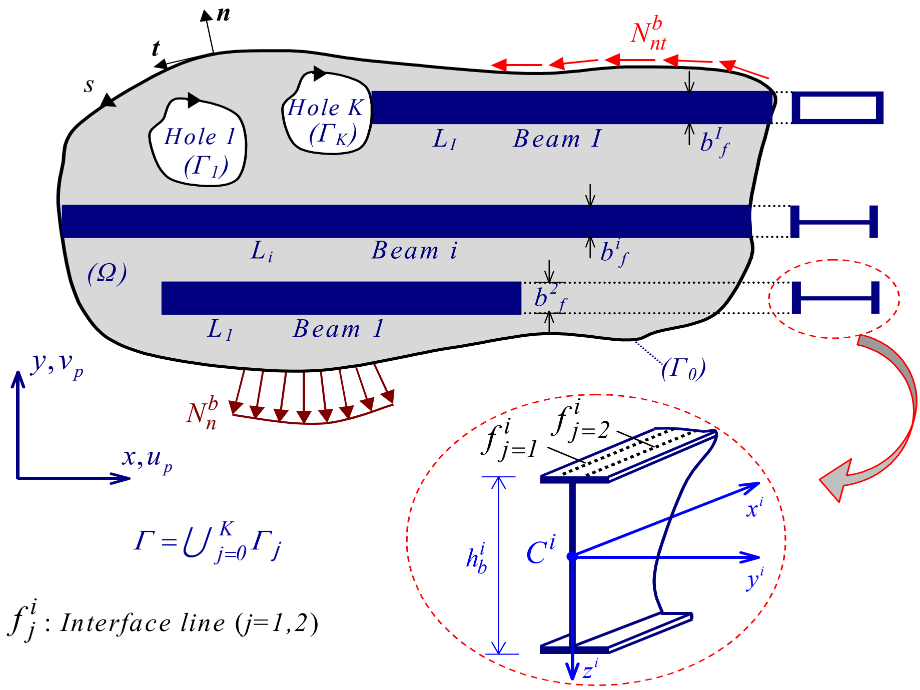

Figure 1: Two dimensional region Ω occupied by the plate

i. A lateral line load q^i_{zj}.

ii. A lateral line load $\partial m^i_{pyj} \big/ \partial x$ due to the eccentricity of the component q^i_{xj} from the middle surface of the plate. $m^i_{pyj} = q^i_{xj} h_p \big/ 2$ is the bending moment.

iii. A lateral line load $\partial m^i_{pxj} \big/ \partial x$ due to the eccentricity of the component q^i_{yj} from the middle surface of the plate. $m^i_{pxj} = q^i_{yj} h_p \big/ 2$ is the bending moment.

iv. An inplane line body force q^i_{xj} at the middle surface of the plate.

v. An inplane line body force q^i_{yj} at the middle surface of the plate.

b. In each (i-th) beam ($\mathbf{O}^i\mathbf{x}^i\mathbf{y}^i\mathbf{z}^i$ *system of axes)*

i. A perpendicularly distributed line load q^i_{zj} along the beam centroid axis $O^i x^i$.

ii. A transversely distributed line load q^i_{yj} along the beam centroid axis $O^i x^i$.

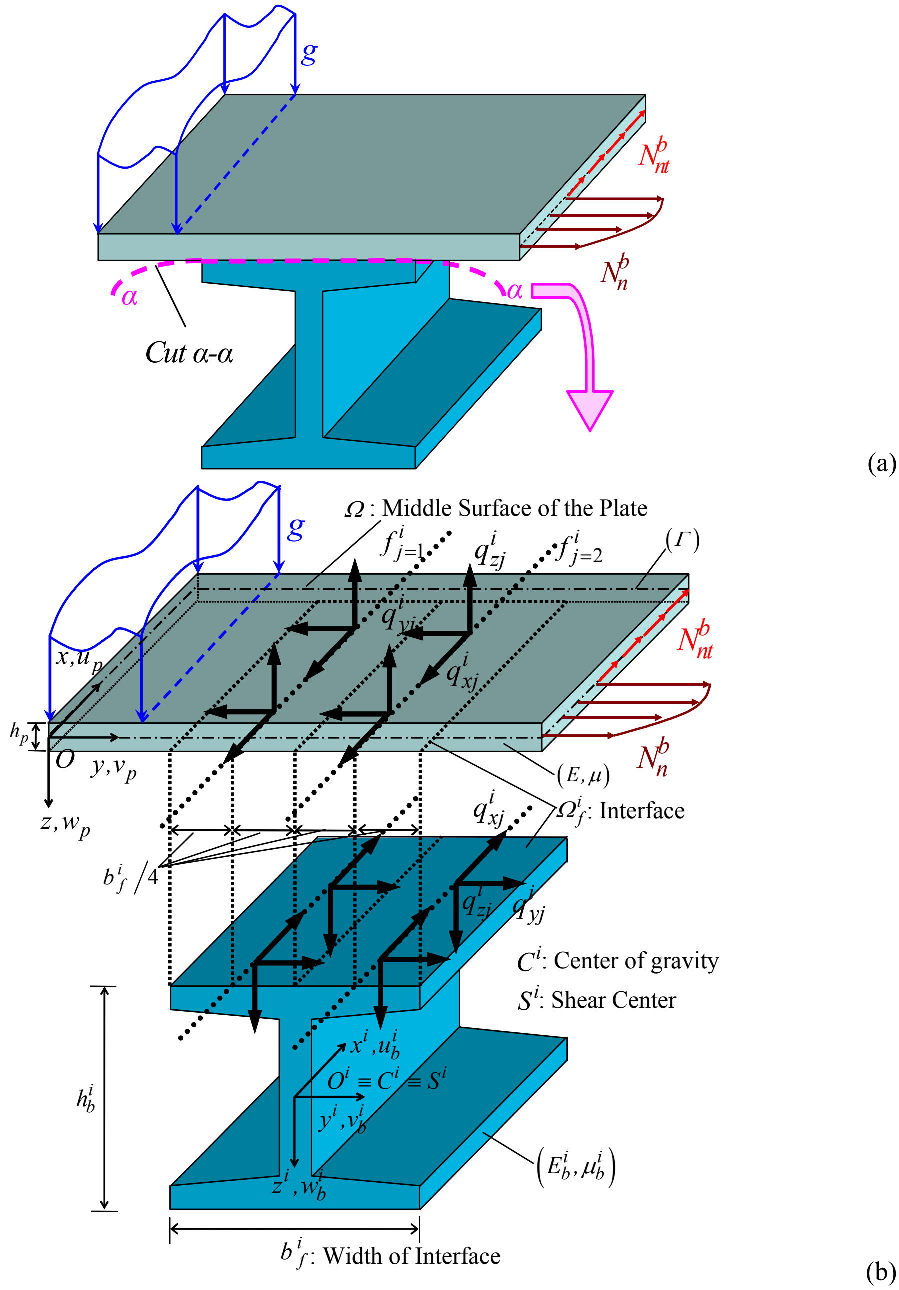

Figure 2: Thin elastic plate stiffened by beams (a) and isolation of the beams from the plate (b)

iii. An axially distributed line load q_{xj}^i along the beam centroid axis $O^i x^i$.

iv. A distributed bending moment $m_{byj}^i = q_{xj}^i e_{zj}^i$ along $O^i y^i$ local beam centroid axis due to the eccentricities e_{zj}^i of the components q_{xj}^i from the beam centroid axis. $e_{z1}^i = e_{z2}^i = -h_b^i/2$ are the eccentricities.

v. A distributed bending moment $m_{bzj}^i = -q_{xj}^i e_{yj}^i$ along $O^i z^i$ local beam centroid axis due to the eccentricities e_{yj}^i of the components q_{xj}^i from the beam centroid axis. $e_{y1}^i = -b_f^i/4$, $e_{y2}^i = b_f^i/4$ are the eccentricities.

vi. A distributed twisting moment $m_{bxj}^i = q_{zj}^i e_{yj}^i - q_{yj}^i e_{zj}^i$ along $O^i x^i$ local beam shear center axis due to the eccentricities e_{zj}^i, e_{yj}^i of the components q_{yj}^i, q_{zj}^i from the beam shear center axis, respectively. $e_{z1}^i = e_{z1}^i = -h_b^i/2$ and $e_{y1}^i = -b_f^i/4$, $e_{y2}^i = b_f^i/4$ are the eccentricities.

The structural models and the aforementioned additional loading of the plate and the beams are shown in Fig.3.

On the base of the above considerations the response of the plate and of the beams may be described by the following initial boundary value problems.

a. For the plate.

The plate undergoes transverse deflection and inplane deformation. Thus, for the transverse deflection the equation of equilibrium employing the linearized second order theory can be written as

$$D\nabla^4 w_p - \left(N_x \frac{\partial^2 w_p}{\partial x^2} + 2N_{xy} \frac{\partial^2 w_p}{\partial x \partial y} + N_y \frac{\partial^2 w_p}{\partial y^2} \right) = \\ g - \sum_{i=1}^{I} \left(\sum_{j=1}^{2} \left(q_{zj}^i - \frac{\partial m_{pxj}^i}{\partial y} + \frac{\partial m_{pyj}^i}{\partial x} - q_{xj}^i \frac{\partial w_{pj}^i}{\partial x} - q_{yj}^i \frac{\partial w_{pj}^i}{\partial y} \right) \delta_j^i (y - y_j) \right) \quad (1)$$

and the corresponding boundary conditions as

$$\alpha_{p1} w_p + \alpha_{p2} R_{pn} = \alpha_{p3} \quad (2a)$$

$$\beta_{p1} \frac{\partial w_p}{\partial n} + \beta_{p2} M_{pn} = \beta_{p3} \text{ on } \Gamma \quad (2b)$$

$$\gamma_{1\mathrm{k}} \mathrm{w}_p + \gamma_{2\mathrm{k}} \left\| \mathrm{Tw}_p \right\|_k = \gamma_{3\mathrm{k}}, \quad \gamma_{2k} \neq 0 \quad (3)$$

where $w_p = w_p(x,y)$ is the transverse deflection of the plate; $D = Eh_p^3/12(1 - \mu^2)$ is its flexural rigidity; $N_x = N_x(x,y)$, $N_y = N_y(x,y)$, $N_{xy} = N_{xy}(x,y)$ are the membrane forces per unit length of the plate cross section arising from the inplane

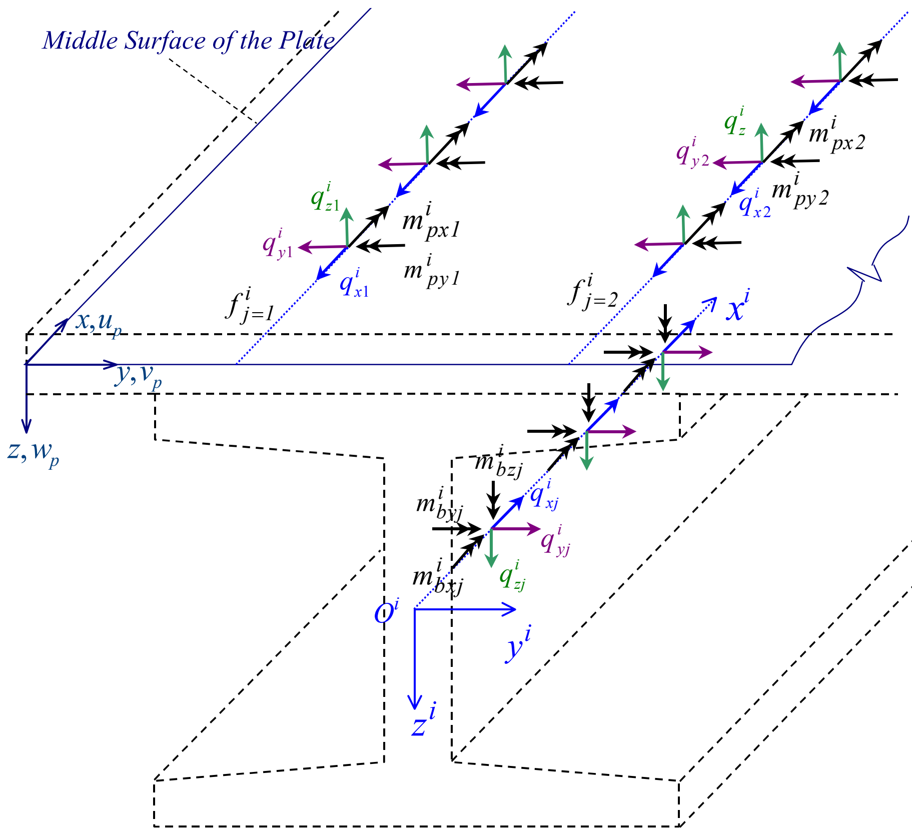

Figure 3: Structural model and directions of the additional loading of the plate and the i-the beam

interface forces q^i_{xj}, q^i_{yj} (i=$1,2,\ldots I$), $(j=1,2)$ and the inplane external boundary loading N^b_n, N^b_{nt}; $\delta(y-y_i)$ is the Dirac's delta function in the y direction; M_{pn}, R_{pn} and Tw_p are the bending moment normal to the boundary, the effective reaction and the twisting moment along it, respectively, which using intrinsic coordinates n, s (Katsikadelis, 1982) are given as

$$M_{pn} = -D\left[\nabla^2 w_p + (\mu-1)\left(\frac{\partial^2 w_p}{\partial s^2} + \kappa\frac{\partial w_p}{\partial n}\right)\right] \tag{4a}$$

$$R_{pn} = -D\left[\frac{\partial}{\partial n}\nabla^2 w_p - (\mu-1)\frac{\partial}{\partial s}\left(\frac{\partial^2 w_p}{\partial s\partial n} - \kappa\frac{\partial w_p}{\partial s}\right)\right] + N_n\frac{\partial w_p}{\partial n} + N_{nt}\frac{\partial w_p}{\partial s} \tag{4b}$$

$$Tw_p = D(\mu-1)\left(\frac{\partial^2 w_p}{\partial s\partial n} - \kappa\frac{\partial w_p}{\partial s}\right) \tag{4c}$$

in which $\kappa = \kappa(s)$ is the curvature of the boundary; $\partial/\partial s$ and $\partial/\partial n$ denote differentiation with respect to the arc length s of the boundary and the outward normal n to it, respectively; N_n, N_{nt} are the boundary membrane forces in the normal and tangential directions to the boundary, respectively, arising from the inplane interface forces q_{xj}^i, q_{yj}^i (i=*1,2,...I*), ($j = 1,2$) and the inplane external boundary loading N_n^b, N_{nt}^b. Finally, $\|\mathrm{Tw}_p\|_k$ is the jump of discontinuity of the twisting moment at the corner point k and a_{pl}, β_{pl}, γ_{ik} ($l = 1,2,3,\ i = 1,2,3$) are functions specified on the boundary Γ. The boundary conditions (2a,b) are the most general boundary conditions for the plate problem including also the elastic support, while the corner condition (3) holds for free or transversely elastically restrained edges k. It is apparent that all types of the conventional boundary conditions (clamped, simply supported, free or guided edge) can be derived form these equations by specifying appropriately the functions a_{pl} and β_{pl} (e.g. for a clamped edge it is $a_{p1} = \beta_{p1} = 1$, $a_{p2} = a_{p3} = \beta_{p2} = \beta_{p3} = 0$).

Since linearized plate bending theory is considered, the components of the membrane forces N_x, N_y, N_{xy} are given as

$$N_x = C\left(\frac{\partial u_p}{\partial x} + \mu\frac{\partial v_p}{\partial y}\right) \tag{5a}$$

$$N_y = C\left(\mu\frac{\partial u_p}{\partial x} + \frac{\partial v_p}{\partial y}\right) \tag{5b}$$

$$N_{xy} = C\frac{1-\mu}{2}\left(\frac{\partial u_p}{\partial y} + \frac{\partial v_p}{\partial x}\right) \tag{5c}$$

where $C = Eh_p/\left(1-\mu^2\right)$; $u_p = u_p(x,y)$, $v_p = v_p(x,y)$ are the displacement components of the middle surface of the plate arising from the inplane interface forces q_{xj}^i, q_{yj}^i (i=*1,2,...I*), ($j = 1,2$) and the inplane external boundary loading N_n^b, N_{nt}^b. These displacement components are established by solving independently the plane stress problem, which is described by the following boundary value problem (Navier's equations of equilibrium)

$$\nabla^2 u_p + \frac{1+\mu}{1-\mu}\frac{\partial}{\partial x}\left[\frac{\partial u_p}{\partial x} + \frac{\partial v_p}{\partial y}\right] - \frac{1}{Gh_p}\sum_{i=1}^{I}\left(\sum_{j=1}^{2} q_{xj}^i \delta_j^i (y - y_i)\right) = 0 \tag{6a}$$

$$\nabla^2 v_p + \frac{1+\mu}{1-\mu}\frac{\partial}{\partial y}\left[\frac{\partial u_p}{\partial x} + \frac{\partial v_p}{\partial y}\right] - \frac{1}{Gh_p}\sum_{i=1}^{I}\left(\sum_{j=1}^{2} q_{yj}^i \delta_j^i (y - y_i)\right) = 0 \text{ in } \Omega \tag{6b}$$

$$\gamma_{p1} u_{pn} + \gamma_{p2} N_n = \gamma_{p3} \tag{7a}$$

$$\delta_{p1} u_{pt} + \delta_{p2} N_{nt} = \delta_{p3} \text{ on } \Gamma \tag{7b}$$

in which $G = E/2(1+\mu)$ is the shear modulus of the plate; u_{pn}, u_{pt} are the displacements in the normal and tangential directions to the boundary, respectively; γ_{pl}, δ_{pl} $(l = 1,2,3)$ are functions specified on the boundary Γ.

b. For each (i-th) beam.

Each beam undergoes transverse deflection with respect to z^i and y^i axes, axial deformation along x^i axis and nonuniform angle of twist along x^i axis. Thus, for the transverse deflection with respect to z^i axis the equation of equilibrium employing the linearized second order theory can be written as

$$E_b^i I_{by}^i \frac{\partial^4 w_b^i}{\partial x^{i4}} = \sum_{j=1}^{2} \left(q_{zj}^i - q_{xj}^i \frac{\partial w_b^i}{\partial x^i} + N_{by}^i \frac{\partial^2 w_b^i}{\partial x^{i2}} - \frac{\partial m_{byj}^i}{\partial x^i} \right) \text{ in } L^i,\ i = 1,2,...,I \tag{8}$$

$$a_1^{zi} w_b^i + a_2^{zi} R_{bz}^i = a_3^{zi} \tag{9a}$$

$$\beta_1^{zi} \theta_{by}^i + \beta_2^{zi} M_{by}^i = \beta_3^{zi} \text{ at the beam ends } x^i = 0, L^i \tag{9b}$$

where $w_b^i = w_b^i\left(x^i\right)$ is the transverse deflection of the i-th beam with respect to z^i axis; I_{by}^i is its bending moment of inertia with respect to y^i axis; $N_{bj}^i = N_{bj}^i\left(x^i\right)$ are the axial forces at the x^i centroid axis arising from the line body forces q_{xj}^i; a_l^{zi}, β_l^{zi} $(l = 1,2,3)$ are coefficients specified at the boundary of the i-th beam; θ_{by}^i, R_{bz}^i, M_{by}^i are the slope, the reaction and the bending moment at the i-th beam ends, respectively given as

$$\theta_{by}^i = -\frac{\partial w_b^i}{\partial x^i} \tag{10}$$

$$R_{bz}^i = -E_b^i I_{by}^i \frac{\partial^3 w_b^i}{\partial x^{i3}} + \sum_{j=1}^{2} N_{bj}^i \frac{\partial w_b^i}{\partial x^i} \tag{11}$$

$$M_{by}^i = -E_b^i I_{by}^i \frac{\partial^2 w_b^i}{\partial x^{i2}} \tag{12}$$

It is apparent that all types of the conventional boundary conditions (clamped, simply supported, free or guided edge) can be derived from eqns (9a,b) by specifying appropriately the coefficients a_l^{zi}, β_l^{zi} (e.g. for a simply supported end it is $a_1^{zi} = \beta_2^{zi} = 1$, $a_2^{zi} = a_3^{zi} = \beta_1^{zi} = \beta_3^{zi} = 0$).

Similarly, the $v_b^i = v_b^i\left(x^i\right)$ transverse deflection with respect to y^i axis must satisfy the following boundary value problem

$$E_b^i I_{bz}^i \frac{\partial^4 v_b^i}{\partial x^{i4}} = \sum_{j=1}^{2} \left(q_{yj}^i - q_{xj}^i \frac{\partial v_b^i}{\partial x^i} + N_{by}^i \frac{\partial^2 v_b^i}{\partial x^{i2}} - \frac{\partial m_{bzj}^i}{\partial x^i} \right) \text{ in } L^i,\ i = 1,2,...,I \tag{13}$$

$$a_1^{yi} v_b^i + a_2^{yi} R_{by}^i = a_3^{yi} \tag{14a}$$

$$\beta_1^{yi} \theta_{bz}^i + \beta_2^{yi} M_{bz}^i = \beta_3^{yi} \text{ at the beam ends } x^i = 0, L^i \tag{14b}$$

where I_{bz}^i is the bending moment of inertia of the i-th beam with respect to y^i axis; a_l^{yi}, β_l^{yi} $(l = 1,2,3)$ are coefficients specified at its boundary; θ_{bz}^i, R_{by}^i, M_{bz}^i are the slope, the reaction and the bending moment at the i-th beam ends, respectively given as

$$\theta_{bz}^i = \frac{\partial v_b^i}{\partial x^i} \tag{15}$$

$$R_{by}^i = -E_b^i I_{bz}^i \frac{\partial^3 v_b^i}{\partial x^{i3}} - \sum_{j=1}^{2} N_{bj}^i \frac{\partial v_b^i}{\partial x^i} \tag{16}$$

$$M_{bz}^i = E_b^i I_{bz}^i \frac{\partial^2 v_b^i}{\partial x^{i2}} \tag{17}$$

Since linearized beam bending theory is considered the axial deformation u_b^i of the beam arising from the arbitrarily distributed axial forces q_{xj}^i (*i=1,2,... I*), $(j = 1,2)$ is described by solving independently the boundary value problem

$$E_b^i A_b^i \frac{\partial^2 u_b^i}{\partial x^{i2}} = -\sum_{j=1}^{2} q_{xj}^i \text{ in } L^i,\ i = 1,2,...,I \tag{18}$$

$$\gamma_1^{xi} u_b^i + \gamma_2^{xi} N_b^i = \gamma_3^{xi} \text{ at the beam ends } x^i = 0, L^i \tag{19}$$

where N_b^i is the axial reaction at the i-th beam ends given as

$$N_b^i = \sum_{j=1}^{2} N_{bj}^i = E_b^i A_b^i \frac{\partial u_b^i}{\partial x_i} \tag{20}$$

Finally, the nonuniform angle of twist with respect to x^i shear center axis has to satisfy the following boundary value problem (Ramm und Hofmann, 1995)

$$E_b^i I_{bw}^i \frac{\partial^4 \theta_{bx}^i}{\partial x^{i4}} - \left(G_b^i I_{bx}^i + \frac{I_{bp}^i}{A_b^i} N_b^i \right) \frac{\partial^2 \theta_{bx}^i}{\partial x^{i2}} + \frac{I_{bp}^i}{A_b^i} \sum_{j=1}^{2} q_{xj}^i \frac{\partial \theta_{bx}^i}{\partial x^i} = \sum_{j=1}^{2} m_{bxj}^i \text{ in } L^i,\ i = 1,2,...,I \tag{21}$$

$$a_1^{xi} \theta_{bx}^i + a_2^{xi} M_{bx}^i = a_3^{xi} \tag{22a}$$

$$\beta_1^{xi}\frac{\partial\theta_{bx}^i}{\partial x^i}+\beta_2^{xi}M_{bw}^i=\beta_3^{xi} \text{ at the beam ends } x_i=0,L_i \tag{22b}$$

where $\theta_{bx}^i=\theta_{bx}^i\left(x^i\right)$ is the variable angle of twist of the i-th beam along the x^i shear center axis; $G_b^i=E_b^i/2(1+\mu_b^i)$ is its shear modulus; $I_{bp}^i=I_{by}^i+I_{bz}^i$ is the polar moment of inertia of the i-th beam; I_{bw}^i, I_{bx}^i are the warping and torsion constants of the i-th beam cross section, respectively given as

$$I_{bw}^i=\int_{A_b^i}\left(\varphi_S^P\right)^2 dA_b^i \tag{23a}$$

$$I_{bx}^i=\int_{A_b^i}\left(\left(y^i\right)^2+\left(z^i\right)^2+y^i\frac{\partial\varphi_S^P}{\partial z^i}-z^i\frac{\partial\varphi_S^P}{\partial y^i}\right)dA_b^i \tag{23b}$$

with $\varphi_S^P\left(y^i,z^i\right)$ the primary warping function with respect to the shear center S of the A_b^i beam cross section (Sapountzakis and Mokos, 2001; Sapountzakis and Mokos, 2003); a_l^{xi}, β_l^{xi} $(l=1,2,3)$ are coefficients specified at the boundary of the i-th beam; $\frac{\partial\theta_{bx}^i}{\partial x^i}$ denotes the rate of change of the angle of twist and it can be regarded as the torsional curvature; M_{bx}^i is the twisting moment and M_{bw}^i is the warping moment due to the torsional curvature at the boundary of the i-th beam given as

$$M_{bx}^i=M_{bx}^{iP}+M_{bx}^{iS} \tag{24a}$$

$$M_{bw}^i=-E_b^iI_{xw}^i\frac{\partial^2\theta_{bx}^i}{\partial x^{i2}} \tag{24b}$$

In eqn (24a) M_{bx}^{iP} is the primary twisting moment resulting from primary shear stress distribution and M_{bx}^{iS} is the secondary twisting moment resulting from secondary shear stress distribution due to warping given as (Sapountzakis and Mokos, 2003)

$$M_{bx}^{iP}=G_b^iI_{bx}^i\frac{\partial\theta_{bx}^i}{\partial x^i} \tag{25a}$$

$$M_{bx}^{iS}=-E_b^iI_{bw}^i\frac{\partial^3\theta_{bx}^i}{\partial x^{i3}} \tag{25b}$$

The boundary conditions (22a,b) are the most general linear torsional boundary conditions for the beam problem including also the elastic support. It is apparent that all types of the conventional torsional boundary conditions (clamped, simply supported, free or guided edge) can be derived form these equations by specifying appropriately the coefficients a_l^{xi}, β_l^{xi} $(l=1,2,3)$ (e.g. for a clamped edge it is $a_1^{xi}=\beta_1^{xi}=1$, $a_2^{xi}=a_3^{xi}=\beta_2^{xi}=\beta_3^{xi}=0$).

Eqns. (1), (6a), (6b), (8), (13), (18), (21) constitute a set of seven coupled partial differential equations including thirteen unknowns, namely w_p, u_p, v_p, w_b^i, v_b^i, u_b^i, θ_{bx}^i, q_{x1}^i, q_{y1}^i, q_{z1}^i, q_{x2}^i, q_{y2}^i, q_{z2}^i. Six additional equations are required, which result from the displacement continuity conditions in the direction of z^i local axes and linear relationships between interface slip and corresponding tractions in the directions of x^i and y^i local axes along the two interface lines of each (i-th) plate – beam interface. These conditions can be expressed as

In the direction of z^i local axis:

$$w_{p1}^i - w_b^i = -\frac{b_f^i}{4}\theta_{bx}^i \text{ along interface line 1 } (f_{j=1}^i) \tag{26a}$$

$$w_{p2}^i - w_b^i = \frac{b_f^i}{4}\theta_{bx}^i \text{ along interface line 2 } (f_{j=2}^i) \tag{26b}$$

In the direction of x^i local axis:

$$u_{p1}^i - u_b^i = \frac{h_p}{2}\frac{\partial w_{p1}^i}{\partial x} + \frac{h_b^i}{2}\frac{\partial w_b^i}{\partial x^i} + \frac{b_f^i}{4}\frac{\partial v_b^i}{\partial x^i} + \left(\phi_S^{iP}\right)_{f1}\frac{\partial \theta_{bx}^i}{\partial x^i} \text{ along interface line 1 } (f_{j=1}^i) \tag{27a}$$

$$u_{p2}^i - u_b^i = \frac{h_p}{2}\frac{\partial w_{p2}^i}{\partial x} + \frac{h_b^i}{2}\frac{\partial w_b^i}{\partial x^i} - \frac{b_f^i}{4}\frac{\partial v_b^i}{\partial x^i} + \left(\phi_S^{iP}\right)_{f2}\frac{\partial \theta_{bx}^i}{\partial x^i} \text{ along interface line 2 } (f_{j=2}^i) \tag{27b}$$

In the direction of y^i local axis:

$$v_{p1}^i - v_b^i = \frac{h_p}{2}\frac{\partial w_{p1}^i}{\partial y} + \frac{h_b^i}{2}\theta_{bx}^i \text{ along interface line 1 } (f_{j=1}^i) \tag{28a}$$

$$v_{p2}^i - v_b^i = \frac{h_p}{2}\frac{\partial w_{p2}^i}{\partial y} + \frac{h_b^i}{2}\theta_{bx}^i \text{ along interface line 2 } (f_{j=2}^i) \tag{28b}$$

where $\left(\phi_S^{iP}\right)_{fj}$ is the value of the primary warping function with respect to the shear center $S$of the beam cross section at the point of the j-th interface line of the i-th plate – beam interface f_j^i. In all the aforementioned equations the values of the primary warping function $\varphi_S^{iP}(y^i, z^i)$ should be set having the appropriate algebraic sign corresponding to the local beam axes. It is worth here noting that the coupling of the aforementioned equations is nonlinear due to the terms including the unknown q_{xj}^i and q_{yj}^i interface forces.

For the buckling problem we assume that the lateral load $g = 0$ and the inplane external boundary loading is expressed in terms of a parameter λ. Thus, the buckling problem is reduced to the following eigenvalue problem

$$
\begin{aligned}
&D\nabla^4 w_p - \left(N_x^q \frac{\partial^2 w_p}{\partial x^2} + 2N_{xy}^q \frac{\partial^2 w_p}{\partial x \partial y} + N_y^q \frac{\partial^2 w_p}{\partial y^2} \right) \\
&= \lambda \left(N_x^b \frac{\partial^2 w_p}{\partial x^2} + 2N_{xy}^b \frac{\partial^2 w_p}{\partial x \partial y} + N_y^b \frac{\partial^2 w_p}{\partial y^2} \right) \\
&\quad - \sum_{i=1}^{I} \left(\sum_{j=1}^{2} \left(q_{zj}^i - \frac{\partial m_{pxj}^i}{\partial y} + \frac{\partial m_{pyj}^i}{\partial x} - q_{xj}^i \frac{\partial w_{pj}^i}{\partial x} - q_{yj}^i \frac{\partial w_{pj}^i}{\partial y} \right) \delta_j^i (y - y_j) \right) \text{ in } \Omega
\end{aligned} \tag{29}
$$

satisfying the boundary conditions

$$\alpha_{p1} w_p + \alpha_{p2} R_{pn} = 0 \tag{30a}$$

$$\beta_{p1} \frac{\partial w_p}{\partial n} + \beta_{p2} M_{pn} = 0 \text{ on } \Gamma \tag{30b}$$

$$\gamma_{1\mathrm{k}} \mathrm{w}_p + \gamma_{2\mathrm{k}} \left\| \mathrm{Tw}_p \right\|_k = 0, \quad \gamma_{2k} \neq 0 \tag{31}$$

where $\left(N_x^q, N_{xy}^q, N_y^q\right)$ and $\left(N_x^b, N_{xy}^b, N_y^b\right)$ are the membrane forces per unit length of the plate cross section arising from the inplane interface forces q_{xj}^i, q_{yj}^i (*i=1,2,… I*), $(j = 1,2)$ and the inplane external boundary loading N_n^b, N_{nt}^b, respectively; M_{pn} and Tw_p are the bending moment normal to the boundary and the twisting moment along it given from the relations (4a) and (4c), respectively, while R_{pn} is the effective reaction given as

$$
\begin{aligned}
R_{pn} = -D &\left[\frac{\partial}{\partial n} \nabla^2 w_p - (\mu - 1) \frac{\partial}{\partial s} \left(\frac{\partial^2 w_p}{\partial s \partial n} - \kappa \frac{\partial w_p}{\partial s} \right) \right] \\
&+ N_n^q \frac{\partial w_p}{\partial n} + N_{nt}^q \frac{\partial w_p}{\partial s} + \lambda \left(N_n^b \frac{\partial w_p}{\partial n} + N_{nt}^b \frac{\partial w_p}{\partial s} \right)
\end{aligned} \tag{32}
$$

The parameter λ is the eigenvalue of the aforementioned eigenvalue problem, while the minimum one is often described as “the buckling factor”. It is the scale factor that must multiply the inplane external boundary loading N_n^b, N_{nt}^b to cause buckling in the given mode. It can also be viewed as a safety factor: if the buckling factor is greater than one, the given loading must be increased to cause buckling; if it is less than one, the loading must be decreased to prevent buckling. The buckling factor can also be negative indicating that buckling will occur if the loading is reversed. Since the first few buckling modes may often have very similar buckling factors, it is recommended that more than one buckling modes have to be taken into account. It is also worth here noting that buckling modes depend upon the loading. There is not one set of buckling modes for the structure in the same way that there is for natural vibration modes. Buckling has to be explicitly evaluated for each set of loading of concern.

3 Solution procedure

The solution of the buckling problem requires the integration of the set of eqns. (6a,b), (8), (13), (18), (21) and (29) subjected to the prescribed boundary conditions. An analytic solution of this problem is out of question. Therefore, the recourse to a numerical solution is inevitable. The method presented by Katsikadelis and Kandilas (1990) as this is applied in Sapountzakis and Mokos (2008) is employed in this investigation. According to this method, the domain Ω occupied by the plate is discretized by establishing a system of M domain nodal points on it, corresponding to M domain cells. Special care is taken so that the nodal points at the interfaces are placed on the traces of the two interface lines of the beams (Fig. 4). Subsequently, the elastic stiffness matrix and the corresponding geometric one of the stiffened plate are established. This procedure leads to the following typical eigenvalue problem (Ramm und Hofmann, 1995)

$$\left[[k]+\lambda\left[k_G\left(N^b\right)\right]\right]\{\phi\}=\{0\} \tag{33}$$

where $[k]$ is the elastic stiffness matrix, $[k_G]$ is the geometric one due to the inplane external boundary loading N_n^b, N_{nt}^b and $\{\phi\}$ is the column matrix of the corresponding eigenvectors–buckling shapes. From eqn. (33) the λ_i $(i=1,2,...,M)$ eigenvalues and the corresponding modeshapes $\{\phi\}_i$ can be established numerically.

a. Elastic stiffness matrix.

For the formulation of the elastic stiffness matrix $[k]$ with respect to the Mdomain nodal points, the elastic flexibility matrix $[f]$ is first established by solving the corresponding static problem working as follows. The typical flexibility coefficient f_{ij} is computed as the static deflection at point i due to a unit lateral load at point$j$. It is apparent that M static solutions are required. The static problem results from the same equations i.e. eqns. (6a,b), (8), (13), (18), (21), (29) under the prescribed boundary conditions and assuming that the parameter $\lambda=0$. The solution of these equations is achieved using the Analog Equation Method (Katsikadelis, 2002; Sapountzakis and Katsikadelis, 2000).

According to this method, applying the biharmonic operator to the function w_p, that is the sought solution of the corresponding boundary value problem described

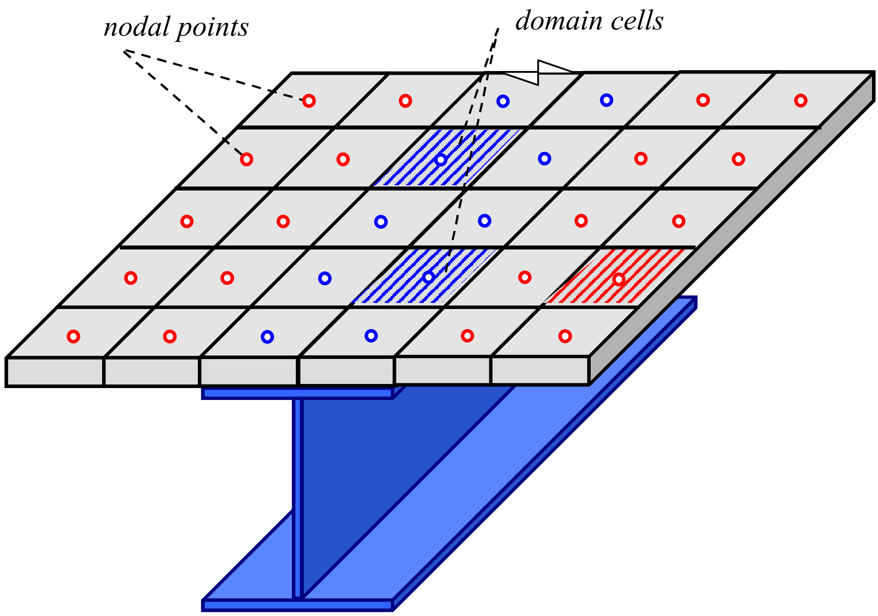

Figure 4: Discretization of the plate

by eqns (1), (30a,b) yields

$$\nabla^4 w_p = p_{pz}(x,y) \tag{34}$$

Eqn (34) indicates that the sought solution can be obtained as the deflection of a plate with unit flexural rigidity subjected to a flexural fictitious load $p_{pz}(x,y)$ under the same boundary conditions. The fictitious load is unknown. Following the formulation developed in (Sapountzakis and Mokos 2007), application of eqn (1) to the M plate nodal points inside Ω and assuming that the stiffened plate is subjected to the lateral load $g = 1$ at point j yields

$$\begin{aligned} &D\{p_{pz}\} - \left([\{N_x^q\}]_{\text{dg.}}[F_{pxx}] + 2\left[\{N_{xy}^q\}\right]_{\text{dg.}}[F_{pxy}] + \left[\{N_y^q\}\right]_{\text{dg.}}[F_{pyy}]\right)\{p_{pz}\} \\ &= \{g\} - [Z]\{q_z\}[Z][X_y]\{q_y\} - [Z][X_x]\{q_x\} + [[Z]\{q_x\}]_{\text{dg.}}[F_{px}]\{p_{pz}\} \\ &\qquad + [[Z]\{q_y\}]_{\text{dg.}}[F_{py}]\{p_{pz}\} \end{aligned} \tag{35}$$

where $\{p_{pz}\}$ is an $M \times 1$ column matrix including the nodal values of the function p_{pz}; $\{g\}$ is an $M \times 1$ column matrix including the unit load at point j; $\left[\{N_x^q\}\right]_{\text{dg.}}$, $\left[\{N_{xy}^q\}\right]_{\text{dg.}}$, $\left[\{N_y^q\}\right]_{\text{dg.}}$ are unknown diagonal $M \times M$ matrices including the membrane values due to the inplane interface forces; $\{q_x\}^T = \{\{q_{x1}\} \quad \{q_{x2}\}\}$, $\{q_y\}^T =$

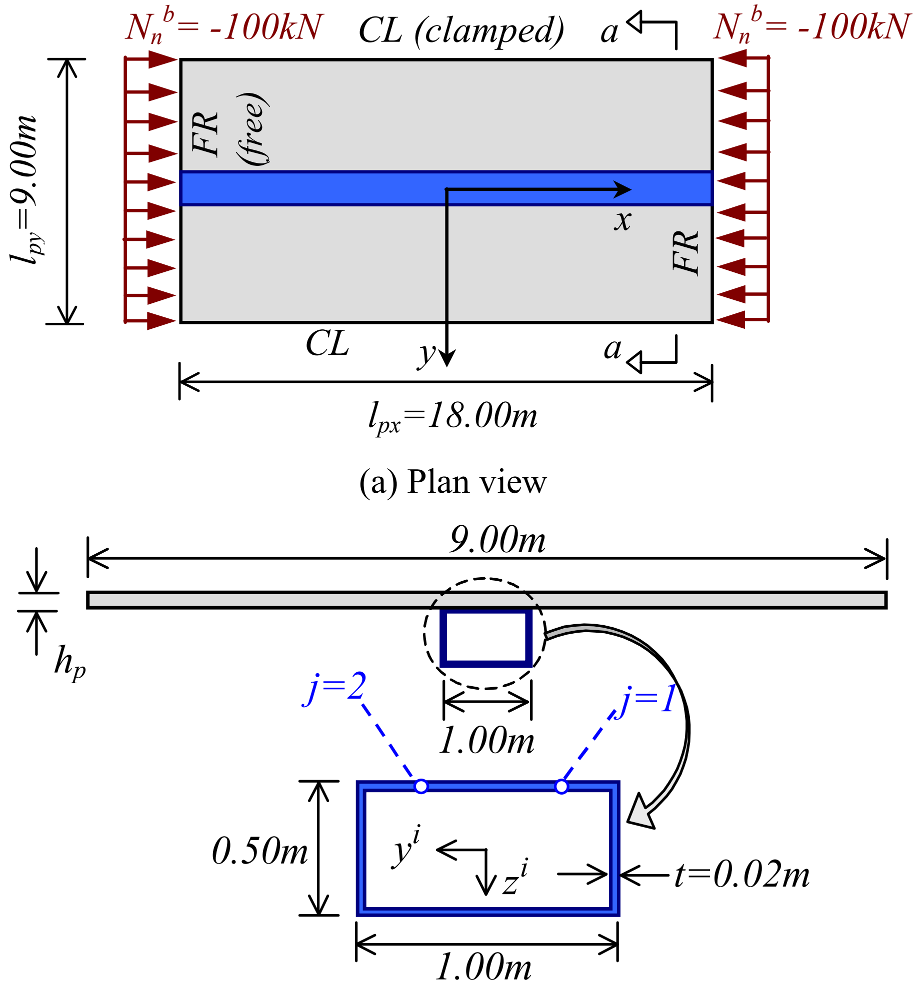

Figure 5: Plan view (a) and section a-a (b) of the stiffened plate of Example 1

$\{\{q_{y1}\} \quad \{q_{y2}\}\}$ and $\{q_z\}^T = \{\{q_{z1}\} \quad \{q_{z2}\}\}$ are vectors with $2L$elements including the unknown q^i_{xj}, q^i_{yj}, q^i_{zj} $(j = 1,2)$ interface forces; $2L$ is the total number of the nodal points at the interfaces; $[Z]$ is a position $M \times 2L$ matrix which converts the vectors $\{q_x\}$, $\{q_y\}$, $\{q_z\}$ into corresponding ones with length M; the symbol $[\,]_{\mathrm{dg.}}$ indicates a diagonal $M \times M$ matrix with the elements of the included column matrix and $[F_{px}]$, $[F_{py}]$, $[F_{pxx}]$, $[F_{pyy}]$, $[F_{pxy}]$ are known $M \times M$ coefficient flexibility matrices (Sapountzakis and Mokos 2007). The matrices $[X_x]$, $[X_y]$ result after approximating the bending moment derivatives of m^i_{pyj}, m^i_{pxj}, respectively using appropriately central, backward, or forward differences. Their dimensions are $2L \times 2L$.

Similarly, differentiating the functions w_b^i, v_b^i, θ_{bx}^i which are the sought solutions of the corresponding boundary value problems described by eqns (8)-(9a,b), (13)-(14a,b) and (21)-(22a,b), respectively, yields

$$\frac{d^4 w_b^i}{dx_i^4} = p_{bz}(x_i) \tag{36a}$$

$$\frac{d^4 v_b^i}{dx_i^4} = p_{by}(x_i) \tag{36b}$$

$$\frac{d^4 \theta_{bx}^i}{dx_i^4} = p_{bx}(x_i) \tag{36c}$$

Eqns (36a,b,c) indicate that the sought solutions can be obtained as the transverse displacements or the angle of twist of a beam with unit flexural or torsional rigidities subjected to flexural or torsional fictitious loads $p_{bz} = p_{bz}\left(x^i\right)$, $p_{by} = p_{by}\left(x^i\right)$, $p_{bx} = p_{bx}\left(x^i\right)$, respectively, under the same boundary conditions. The fictitious loads are unknown. Following the formulation developed in (Sapountzakis and Mokos 2007), application of the eqn (8) to the $2L$ nodal points in the interior of the beams yields

$$\begin{aligned}\left(E_b^i I_{by}^i [I] - \left[\left\{N_b^i\right\}\right]_{\text{dg.}} \left[F_{bxx}^z\right] + \left[\{q_{x1}\} + \{q_{x2}\}\right]_{\text{dg.}} \left[F_{bx}^z\right]\right)\{p_{bz}\} = \{q_{z1}\} + \{q_{z2}\} \\ + [X_{bx}]\left(\{q_{x1}\} + \{q_{x2}\}\right)\end{aligned} \tag{37}$$

while similarly application of the eqn (13) gives

$$\begin{aligned}\left(E_b^i I_{bz}^i [I] - \left[\left\{N_b^i\right\}\right]_{\text{dg.}} \left[F_{bxx}^y\right] + \left[\{q_{x1}\} + \{q_{x2}\}\right]_{\text{dg.}} \left[F_{bx}^y\right]\right)\{p_{by}\} = \{q_{y1}\} + \{q_{y1}\} \\ - \quad \left[X_{by}\right]\left(\{q_{y1}\} + \{q_{y2}\}\right)\end{aligned} \tag{38}$$

and for the angle of twist θ_{bx}^i application of the eqn (21) yields

$$\begin{aligned}\left(E_b^i I_{bw}^i [I] - \left(G_b^i I_{bx}^i [I] + \frac{I_{bp}^i}{A_b^i}\left[\left\{N_b^i\right\}\right]_{\text{dg.}}\right)\left[F_{bxx}^x\right] + \frac{I_{bp}^i}{A_b^i}\left[\{q_{x1}\} + \{q_{x2}\}\right]_{\text{dg.}}\left[F_{bx}^x\right]\right)\{p_{bx}\} \\ = [e_{y1}]\{q_{z1}\} + [e_{y2}]\{q_{z2}\} - [e_{z1}]\{q_{y1}\} - [e_{z2}]\{q_{y2}\}\end{aligned} \tag{39}$$

where $\left[\left\{N_b^i\right\}\right]_{\text{dg.}}$ is an unknown diagonal $L \times L$ matrix including the values of the axial forces; the symbol $[]_{\text{dg.}}$ indicates a diagonal $L \times L$ matrix with the elements of the included column matrix. The matrices $[X_{bx}]$, $\left[X_{by}\right]$ result after approximating the derivatives of m_{byj}^i, m_{bzj}^i using appropriately central, backward, or forward differences. Their dimensions are also $L \times L$. Moreover, $\{p_{bz}\}$, $\{p_{by}\}$, $\{p_{bx}\}$ are $L \times 1$ column matrices including the values of the fictitious flexural and torsional loading, $[F_{bx}^{y}]$, $[F_{bxx}^{y}]$, $[F_{bx}^{z}]$, $[F_{bxx}^{z}]$, $[F_{bx}^{x}]$, $[F_{bxx}^{x}]$ are $L \times L$ flexibility coefficient matrices, while $[e_{y1}]$, $[e_{y2}]$, $[e_{z1}]$, $[e_{z2}]$ are diagonal $L \times L$ matrices including the values of the eccentricities e_{yj}^{i}, e_{zj}^{i} of the components q_{zj}^{i}, q_{yj}^{i} with respect to the i-th beam shear center axis, respectively.

Moreover, using the same boundary discretization and solving the inplane plate problem (6a,b)-(7a,b), by using the BEM (Katsikadelis, 2002), for each nodal interface point separately for $q_{xj}^{i} = 1.0$ and $q_{yj}^{i} = 1.0$ $(j = 1,2)$, the descretized $2L$ values of the nodal membrane forces for homogeneous boundary conditions (7a,b) $(\gamma_{p3} = \delta_{p3} = 0)$ are expressed as follows

$$\{N_x^q\} = [G_{dx}^x]\{q_x\} + [G_{dx}^y]\{q_y\} \tag{40a}$$

$$\{N_{xy}^q\} = [G_{dxy}^x]\{q_x\} + [G_{dxy}^y]\{q_y\} \tag{40b}$$

$$\{N_y^q\} = [G_{dy}^x]\{q_x\} + [G_{dy}^y]\{q_y\} \tag{40c}$$

while the descretized L values of the nodal displacement components of the middle surface of the plate are given as

$$\{u_{p1}\} = [F_{d1}^{xx}]\{q_{x1}\} + [F_{d1}^{xy}]\{q_{y1}\} \tag{41a}$$

$$\{u_{p2}\} = [F_{d2}^{xx}]\{q_{x2}\} + [F_{d2}^{xy}]\{q_{y2}\} \tag{41b}$$

$$\{v_{p1}\} = [F_{d1}^{yx}]\{q_{x1}\} + [F_{d1}^{yy}]\{q_{y1}\} \tag{41c}$$

$$\{v_{p2}\} = [F_{d2}^{yx}]\{q_{x2}\} + [F_{d2}^{yy}]\{q_{y2}\} \tag{41d}$$

where $[G_{dx}^x]$, $[G_{dx}^y]$, $[G_{dxy}^x]$, $[G_{dxy}^y]$, $[G_{dy}^x]$, $[G_{dy}^y]$ are known matrices with dimensions $M \times 2L$ and $[F_{d1}^{xx}]$, $[F_{d2}^{xx}]$, $[F_{d1}^{xy}]$, $[F_{d2}^{xy}]$, $[F_{d1}^{yx}]$, $[F_{d2}^{yx}]$, $[F_{d1}^{yy}]$, $[F_{d2}^{yy}]$ are known flexibility matrices with dimensions $L \times L$. Similarly, the descretized L values of the nodal axial forces and the nodal displacements at the beam centroid axis for homogeneous boundary conditions (19) $(\gamma_3^{xi} = 0)$ can be expressed as

$$\{N_b^i\} = [G_b^x](\{q_{x1}\} + \{q_{x2}\}) \tag{42a}$$

$$\{u_b^i\} = [F_b^x](\{q_{x1}\} + \{q_{x2}\}) \tag{42b}$$

where $[G_b^x]$, $[F_b^x]$ are known $L \times L$ matrices.

Eqns (35), (37), (38), (39) after elimination of the quantities N_x^q, N_y^q, N_{xy}^q, N_b^i using eqns (40a,b,c), (42a) together with continuity conditions (26a,b), (27a,b), (28a,b) which employing eqns. (30a,b,c,d), (42a) and after discretization at the L nodal points at the interfaces are written as

$$[Y_1][F_p]\{p_{pz}\} - \left[F_b^z\right]\{p_{bz}\} = -\frac{b_f^i}{4}\left[F_b^t\right]\{p_{bx}\} \tag{43a}$$

$$[Y_2][F_p]\{p_{pz}\} - \left[F_b^z\right]\{p_{bz}\} = \frac{b_f^i}{4}\left[F_b^t\right]\{p_{bx}\} \tag{43b}$$

$$\begin{aligned}&\left[F_{d1}^{xx}\right]\{q_{x1}\} + \left[F_{d1}^{xy}\right]\{q_{y1}\} - \left[F_b^x\right](\{q_{x1}\} + \{q_{x2}\}) = \\ &\quad \frac{h_p}{2}[Y_1][F_{px}]\{p_{pz}\} + \frac{h_b^i}{2}\left[F_{bx}^z\right]\{p_{bz}\} + \frac{b_f^i}{4}\left[F_{bx}^y\right]\{p_{by}\} + \left(\phi_S^P\right)_{f_1^i}\left[F_b^t\right]\{p_{bx}\}\end{aligned} \tag{44a}$$

$$\begin{aligned}&\left[F_{d2}^{xx}\right]\{q_{x2}\} + \left[F_{d2}^{xy}\right]\{q_{y2}\} - \left[F_b^x\right](\{q_{x1}\} + \{q_{x2}\}) = \\ &\quad \frac{h_p}{2}[Y_2][F_{px}]\{p_{pz}\} + \frac{h_b^i}{2}\left[F_{bx}^z\right]\{p_{bz}\} - \frac{b_f^i}{4}\left[F_{bx}^y\right]\{p_{by}\} + \left(\phi_S^P\right)_{f_2^i}\left[F_b^t\right]\{p_{bx}\}\end{aligned} \tag{44b}$$

$$\left[F_{d1}^{yx}\right]\{q_{x1}\} + \left[F_{d1}^{yy}\right]\{q_{y1}\} - \left[F_b^y\right]\{p_{bz}\} = \frac{h_p}{2}[Y_1][F_{py}]\{p_{pz}\} + \frac{h_p}{2}\left[F_b^t\right]\{p_{bx}\} \tag{45a}$$

$$\left[F_{d2}^{yx}\right]\{q_{x2}\} + \left[F_{d2}^{yy}\right]\{q_{y2}\} - \left[F_b^y\right]\{p_{bz}\} = \frac{h_p}{2}[Y_2][F_{py}]\{p_{pz}\} + \frac{h_p}{2}\left[F_b^t\right]\{p_{bx}\} \tag{45b}$$

constitute a non-linear system of ten equations with respect to $\{q_{x1}\}$, $\{q_{x2}\}$, $\{q_{y1}\}$, $\{q_{y2}\}$, $\{q_{z1}\}$, $\{q_{z2}\}$ (interface forces) and $\{p_{pz}\}$, $\{p_{bx}\}$, $\{p_{by}\}$, $\{p_{bz}\}$ (fictitious loading of plate and beams). This system is solved using iterative numerical methods. Note that $[F_p]$, $\left[F_b^z\right]$, $\left[F_b^t\right]$, $\left[F_{d1}^{xx}\right]$, $\left[F_{d2}^{xx}\right]$, $\left[F_{d1}^{xy}\right]$, $\left[F_{d2}^{xy}\right]$, $\left[F_{d1}^{yx}\right]$, $\left[F_{d1}^{yy}\right]$, $\left[F_b^x\right]$, $\left[F_b^y\right]$, $[F_{px}]$, $[F_{py}]$, $\left[F_{bx}^z\right]$, $\left[F_{bx}^y\right]$ are known flexibility coefficient matrices with dimensions $L\times L$, while and $[Y_1]$, $[Y_2]$ are position $L\times M$ matrices which convert the matrices $[F_p]$, $[F_{px}]$, $[F_{py}]$ into corresponding ones with dimensions $L\times M$, appropriately referring to the nodal points of the two interface lines $f_{j=1}^i$, $f_{j=2}^i$, respectively.

Thus, after Mstatic solutions the elastic flexibility matrix $[f]$ is formulated, while the elastic stiffness matrix of the stiffened plate $[k]$ is obtained by inverting the elastic flexibility matrix $[f]$. It is worth here noting that the elastic stiffness matrix $[k]$ depends on the interface forces q_{xj}^i, q_{yj}^i and is independent of the inplane external boundary loading N_n^b, N_{nt}^b since the parameter $\lambda = 0$.

b. Geometric stiffness matrix.

For the formulation of the geometric stiffness matrix $[k_G]$, two additional elastic stiffness matrices $\left[k^0\right]$, $\left[k^1\right]$ have to be established, for which the corresponding flexibility matrices $\left[f^0\right]$, $\left[f^1\right]$ are priorly formulated, by solving the corresponding static problems by working similarly with the presented method for the flexibility matrix $[f]$ in the previous section. The static problems result from the equations (6a,b), (8), (13), (18), (21), (29) under the prescribed boundary conditions and ignoring the interface forces, that is $q_{xj}^{i} = q_{yj}^{i} = 0$, where for the flexibility matrix $\left[f^{0}\right]$ the parameter $\lambda = 0$ and for the flexibility matrix $\left[f^{1}\right]$ the parameter $\lambda = 1$. As soon as the flexibility matrices $\left[f^{0}\right]$, $\left[f^{1}\right]$ are established the two required additional elastic stiffness matrices $\left[k^{0}\right]$, $\left[k^{1}\right]$ are obtained by inverting the aforementioned flexibility matrices. Finally, the geometric stiffness matrix $[k_{G}]$ is given as

$$[k_{G}] = \left[k^{1}\right] - \left[k^{0}\right] \tag{46}$$

It is worth here noting that for the calculation of the flexibility matrices $\left[f^{0}\right]$, $\left[f^{1}\right]$ the system of the equations is linear since the interface forces are ignored.

Finally, in the aforementioned presented model the case of deformable connection between the plate and the beams can also be taken into account by adding at the right hand side of the eqns (27a,b) and eqns (28a,b) the additional terms $q_{xj}^{i}k_{xj}^{i}$ and $q_{yj}^{i}k_{yj}^{i}$, respectively, where

,

are the stiffnesses of the arbitrarily distributed shear connectors along x_i and y_i directions, respectively.

4 Numerical examples

On the basis of the analytical and numerical procedures presented in the previous sections, a FORTRAN program has been written and representative examples have been studied to demonstrate the efficiency and the range of applications of the developed method. In all the examples treated $E = 3.00 \times 10^{7} kN/m^{2}$, $\mu = 0.20$ and $E_{b}^{i} = 2.10 \times 10^{8} kN/m^{2}$, $\mu_{b}^{i} = 0.30$, while the numerical results have been obtained using 180 constant boundary elements and 324 constant domain rectangular cells.

Example 1

A concrete rectangular plate with dimensions $l_{px} \times l_{py} = 18.0 \times 9.0\ m$ stiffened by a hollow rectangular steel beam (Fig.5) symmetrically placed has been studied. The plate is clamped along its long edges, while the other two small edges are free according to both its transverse and inplane boundary conditions. The steel beam is also clamped at its edges according to its transverse, axial and torsional boundary conditions. The plate is uniformly compressed in the x direction, that is $N_{n}^{b} = -100kN$ and $N_{nt}^{b} = 0$ at $x = l_{px}/2$, $x = -l_{px}/2$ (Fig.5).

In Table 1 the computed buckling factor λ_1 of the stiffened plate for various values of the plate thickness h_p taking into account or ignoring the interface forces

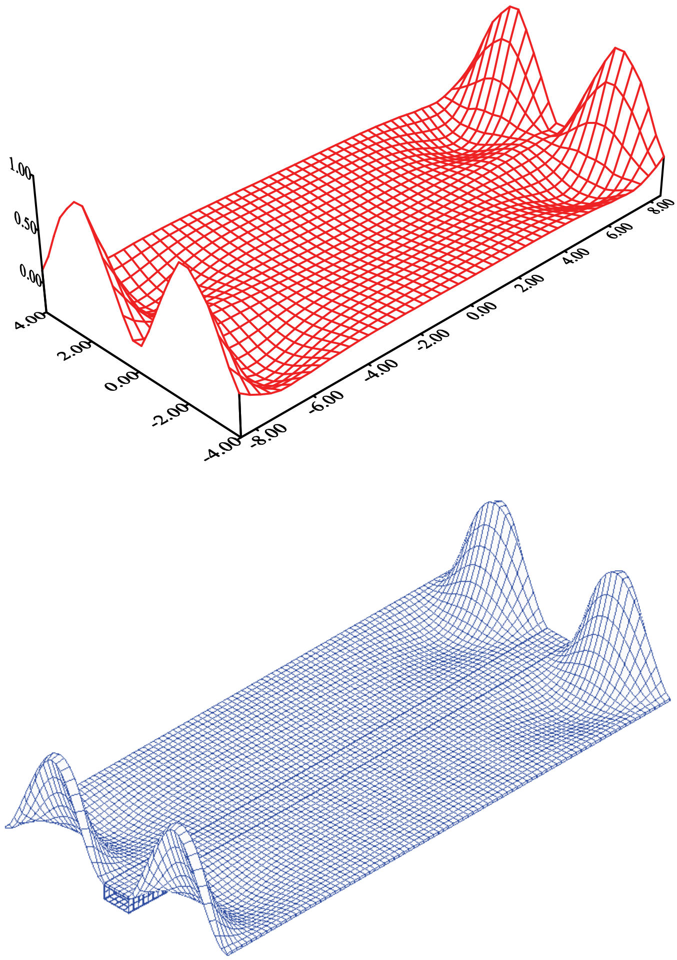

$\lambda_I = 29.7872$

(a)

$\lambda_I = 31.6443$
(MSC/NASTRAN
for Windows, 1999)

(b)

Figure 6: First buckling modeshape surface for plate thickness $h_p = 8cm$ using the proposed method (a) and a FEM solution (b) of the stiffened plate of Example 1

q^i_{xj}, q^i_{yj} are presented as compared with those obtained from a 3–D FEM solution (MSC/NASTRAN for Windows, 1999) using 5850 8-noded hexahedral solid finite elements (parabolic elements). Moreover, in Fig.6 the first buckling modeshape surface for the plate thickness $h_p = 8cm$ using the proposed method and the aforementioned solid FE solution are presented, while the contour lines of the first buckling modeshape for the plate thickness $h_p = 5cm$ and $h_p = 12cm$ are shown in Fig.7. From Table 1 and Fig.6 the accuracy of the results and the validity of the

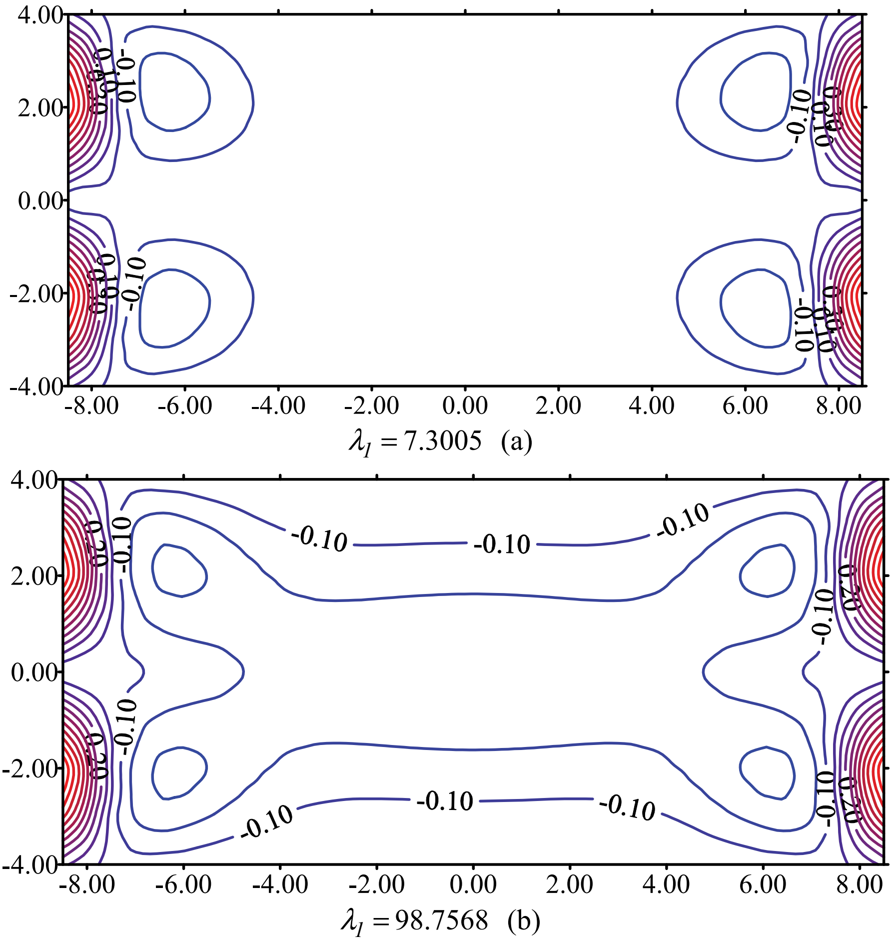

Figure 7: Contour lines of the first buckling modeshape for plate thickness $h_p = 5cm$ (a) and $h_p = 12cm$ (b) of the stiffened plate of Example 1

proposed model are concluded, while form Table 1 and Fig.7 the increment of the buckling factor with the increment of the plate thickness is easily verified.

Example 2

As a second example a concrete rectangular plate with dimensions $l_{px} \times l_{py} = 18.0 \times 9.0\ m$ stiffened by a hollow rectangular steel beam eccentrically placed with respect to the centerline of the plate has been studied (Fig.8). The plate is clamped along its one long edge, while the other three edges are free according to both its transverse and inplane boundary conditions. The steel beam is also clamped at

Table 1: Buckling factor λ_1 of the stiffened plate of Example 1 for various plate thickness h_p.

h_p	AEM		3–D FEM
	Without interface forces $q_{xj}^i,\ q_{yj}^i = 0$	With interface forces $q_{xj}^i,\ q_{yj}^i \neq 0$ (Present study)	Solid FE (MSC/NASTRAN for Windows, 1999)
5	7.2950	7.3005	7.8458
6	12.5913	12.6164	13.4949
7	19.9333	20.0049	21.3194
8	29.6202	29.7872	31.6443
9	41.9309	42.2707	44.7793
10	57.1215	57.7476	61.0183
11	75.4246	76.4914	80.6387
12	97.0479	98.7568	103.9009

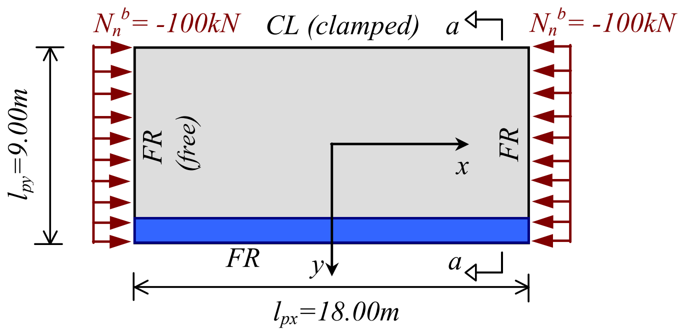

(a) Plan view

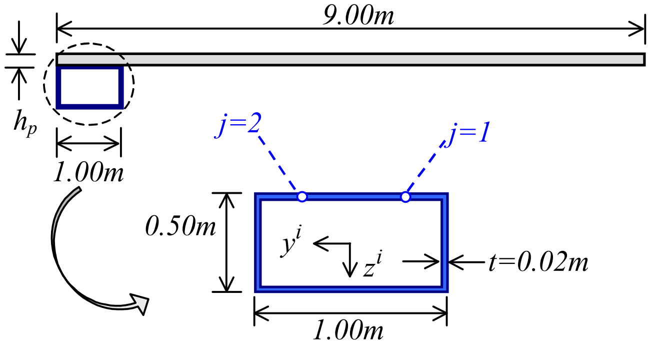

$I_{bx}^i = 6.14016E-03m^4$, $I_{bw}^i = 3.29566E-05m^6$, $\left(\phi_S^P\right)_{f1} = -\left(\phi_S^P\right)_{f2} = -2.5832E-02m^2$

(b) Section *a-a*

Figure 8: Plan view (a) and section a-a (b) of the stiffened plate of Example 2

its edges according to its transverse, axial and torsional boundary conditions. The plate is uniformly compressed in the x direction, that is $N_n^b = -100kN$ and $N_{nt}^b = 0$ at $x = l_{px}/2$, $x = -l_{px}/2$ (Fig.8).

In Table 2 the obtained buckling factor λ_1 of the stiffened plate for various values of the plate thickness h_p taking into account or ignoring the interface forces q_{xj}^i, q_{yj}^i are presented as compared with those obtained from a 3–D FEM solution (MSC/NASTRAN for Windows, 1999) using 5850 8-noded hexahedral solid finite elements (parabolic elements). Furthermore, in Fig.9 the first buckling modeshape surface for the plate thickness $h_p = 10cm$ using the proposed method and the aforementioned FE solution are presented. From Table 2 and Fig.9 the accuracy of the results and the validity of the proposed model are once more verified. Moreover, in Fig.10 for the plate thickness $h_p = 8cm$ the total interface forces q_x, q_y, q_z along the axis of the beam of the stiffened plate are also presented.

Table 2: Buckling factor λ_1 of the stiffened plate of Example 2, for various values of the plate thickness h_p.

h_p	AEM		3–D FEM
	Without interface forces $q^i_{xj},\ q^i_{yj}=0$	With interface forces $q^i_{xj},\ q^i_{yj}\neq 0$ (Present study)	Solid FE (MSC/NASTRAN for Windows, 1999)
8	8.2280	8.2000	8.0620
9	11.6964	11.6390	11.4373
10	16.0128	15.9047	15.6262
11	21.2629	21.0715	20.7079
12	27.5290	27.2065	26.7590
13	34.8899	34.2770	33.8531
14	43.4200	42.1927	42.0522
15	53.1901	51.0244	51.4520

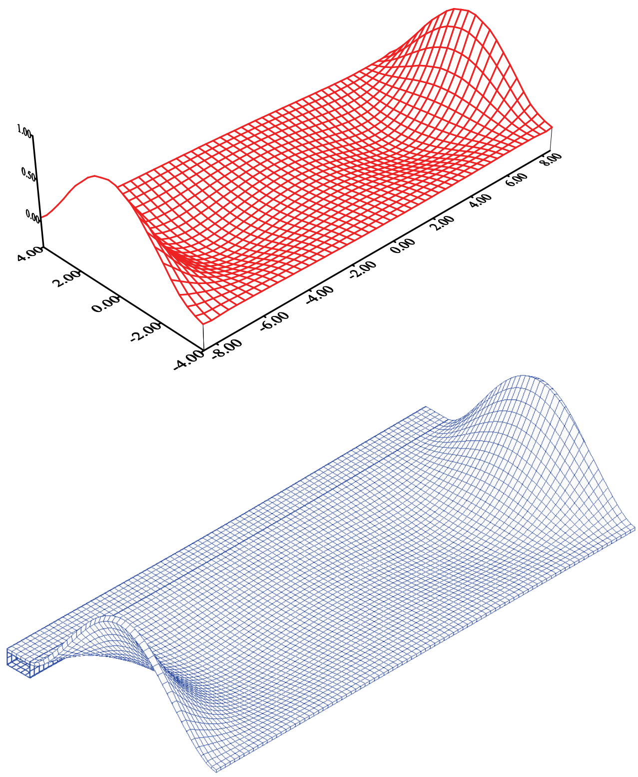

$\lambda_1 = 8.2000$

(a)

$\lambda_1 = 8.0620$

(MSC/NASTRAN for Windows, 1999)

(b)

Figure 9: First buckling modeshape surface for plate thickness $h_p = 10cm$ using the proposed method (a) and a FEM solution (b) of the stiffened plate of Example 2

Example 3

As a final example, a concrete rectangular plate with dimensions $l_{px} \times l_{py} = 18.0 \times 9.0\ m$ stiffened by two identical I-section steel beams, as this is presented in Fig.11 has been studied. The plate is clamped along its small two edges, while the other two long edges are free according to both its transverse and inplane boundary conditions. The steel beams are also clamped at its edges according to its transverse, axial and torsional boundary conditions. The plate is uniformly compressed in the y direction, that is $N_n^b = -100kN$ and $N_{nt}^b = 0$ at $y = l_{py}/2$, $y = -l_{py}/2$ (Fig.11).

In Table 3 the obtained buckling factor λ_1 of the stiffened plate for various values of the plate thickness h_p taking into account or ignoring the interface forces q_{xj}^i, q_{yj}^i are presented as compared with those obtained from a 3–D FEM solution ((MSC/NASTRAN for Windows, 1999) using 6750 8-noded hexahedral solid finite

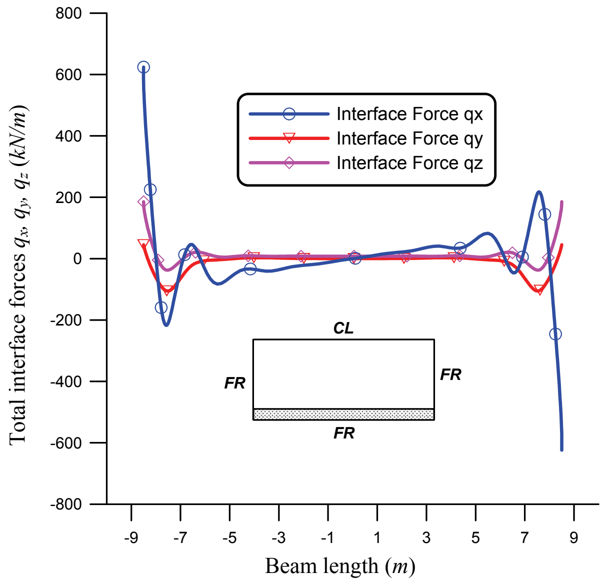

Figure 10: Total interface forces q_x, q_y, q_z along the axis of the beam of the stiffened plate of Example 2, for boundary loading $N_n^b = -100kN$ and plate thickness $h_p = 8cm$

elements (parabolic elements). Moreover, in Fig.12 the first three buckling mode-shape surfaces for the plate thickness $h_p = 12cm$ are presented using the proposed method and the aforementioned solid FE solution. From this table and figure the validity of the proposed model is once more concluded. Finally, for the boundary loading $N_n^b = -100kN$ and plate thickness $h_p = 12cm$, in Fig.13 the total interface forces q_x, q_y, q_z, in Fig.14 the transverse deflection w_b^i, v_b^i, in Fig.15 the twisting M_{bx}^i and warping M_{bw}^i moments and in Fig.16 the bending moments M_{by}^i and M_{bz}^i, along the axes of the beams of the stiffened plate are presented, respectively.

5 Concluding remarks

A general solution for the buckling analysis of plates stiffened by arbitrarily placed parallel beams of arbitrary doubly symmetric cross section subjected to an arbitrary inplane loading using a BEM-based method is presented. The proposed model is an improved one, which contrary to previous approaches, takes into account the nonuniform distribution of the interface transverse shear force and the nonuniform torsional response of the beams. The main conclusions that can be drawn from this investigation are

Table 3: Buckling factor λ_1 of the stiffened plate of Example 3, for various values of the plate thickness h_p.

h_p	AEM		3–D FEM
	Without interface forces $q_{xj}^i, q_{yj}^i = 0$	With interface forces $q_{xj}^i, q_{yj}^i \neq 0$ (Present study)	Solid FE (MSC/NASTRAN for Windows, 1999)
8	3.1091	3.7627	3.8925
9	4.1834	4.9663	5.2318
10	5.5099	6.4129	6.8703
11	7.1202	8.1370	8.8410
12	9.0449	10.1762	11.1757
13	11.3137	12.5571	13.9040
14	13.9561	15.3145	17.0612
15	17.0014	18.4887	20.6725

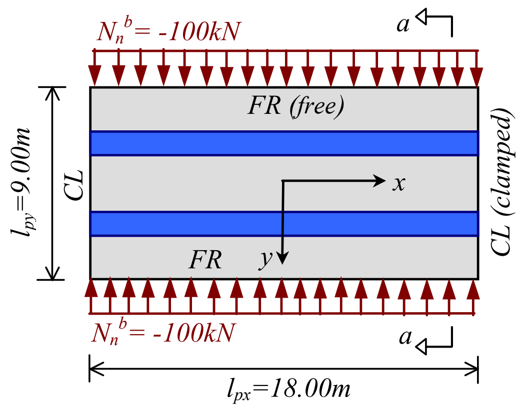

(a) Plan view

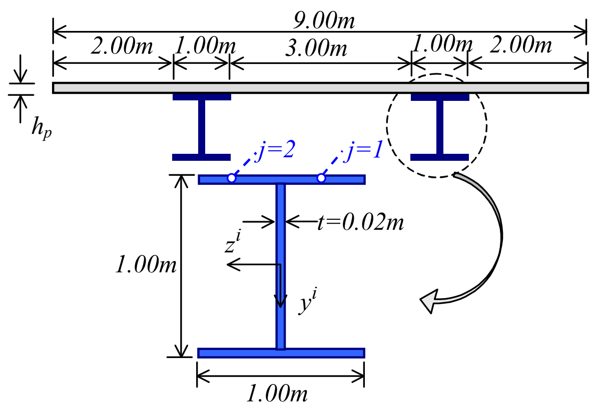

$I_{bx}^i = 8.09899E-06m^4$, $I_{bw}^i = 7.96197E-04m^6$, $\left(\phi_S^P\right)_{f1} = -\left(\phi_S^P\right)_{f2} = 1.1862E-01m^2$

(b) Section *a-a*

Figure 11: Plan view (a) and section a-a (b) of the stiffened plate of Example 3

a. The validity of the proposed model and the accuracy of the results compared with those obtained from a 3–D FEM solution are noteworthy.

b. The increment of the buckling factor with the increment of the plate thickness is easily verified.

c. The influence of the inplane interface forces in the value of the buckling factor is also concluded.

d. The adopted model permits the evaluation of the shear forces at the interfaces in both directions for stiffened plates subjected to inplane loading, the knowledge

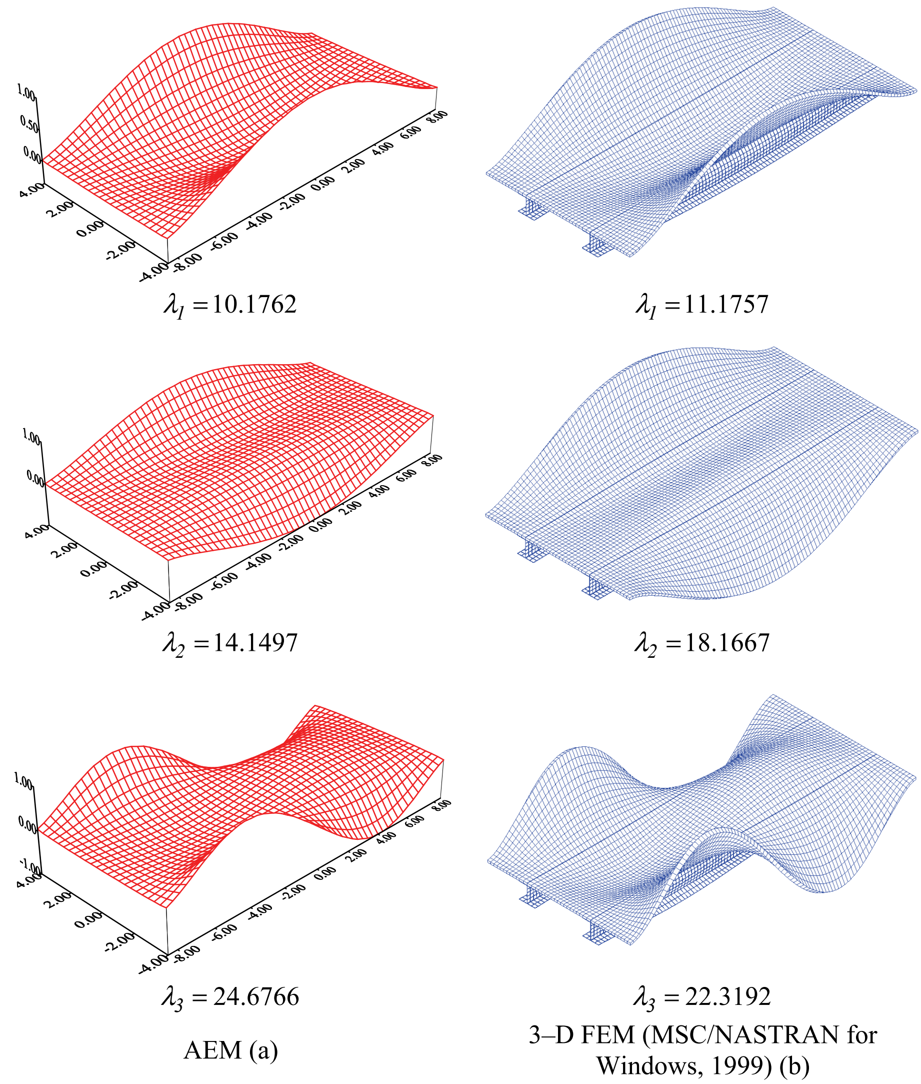

Figure 12: First three buckling modeshape surfaces for plate thickness $h_p = 12cm$ using the proposed method (a) and a FEM solution (b) of the stiffened plate of Example 3

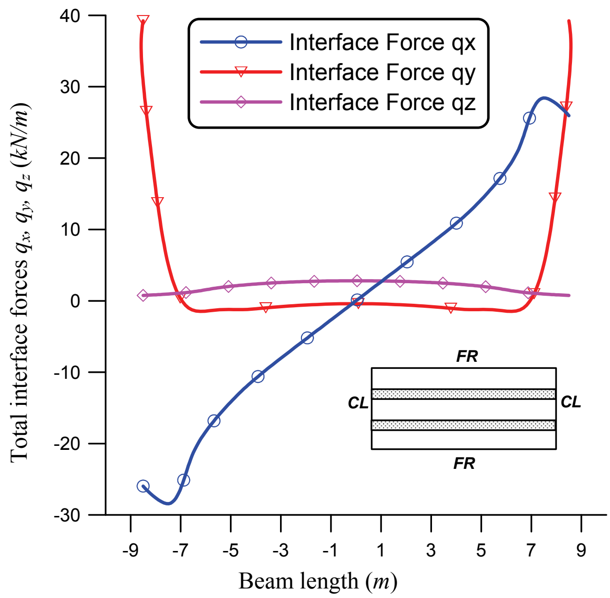

Figure 13: Total interface forces q_x, q_y, q_z along the axis of the beams of the stiffened plate of Example 3

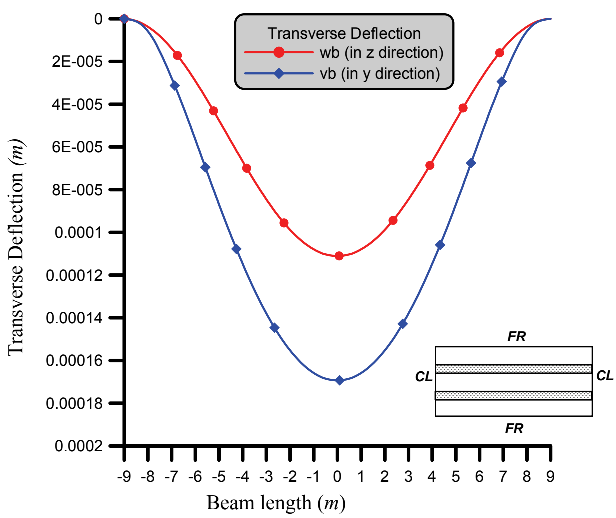

Figure 14: Transverse deflection w_b^i, v_b^i along the axis of the beams of the stiffened plate of Example 3

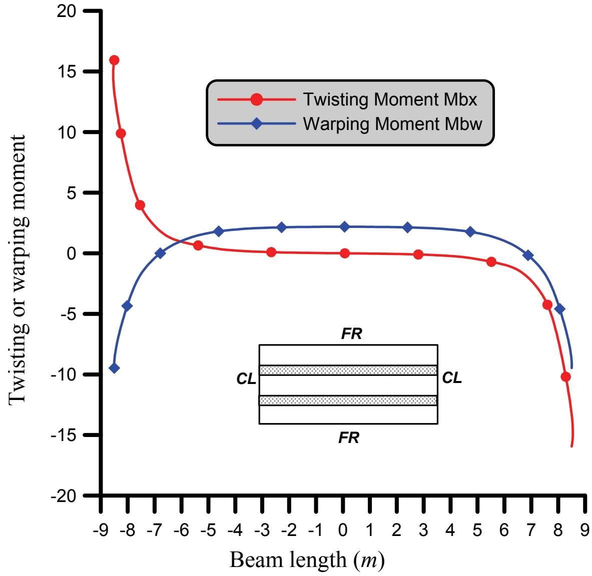

Figure 15: Twisting M_{bx}^{i} (kNm) and warping M_{bw}^{i} (kNm^2) moments along the axis of the beams of the stiffened plate of Example 3

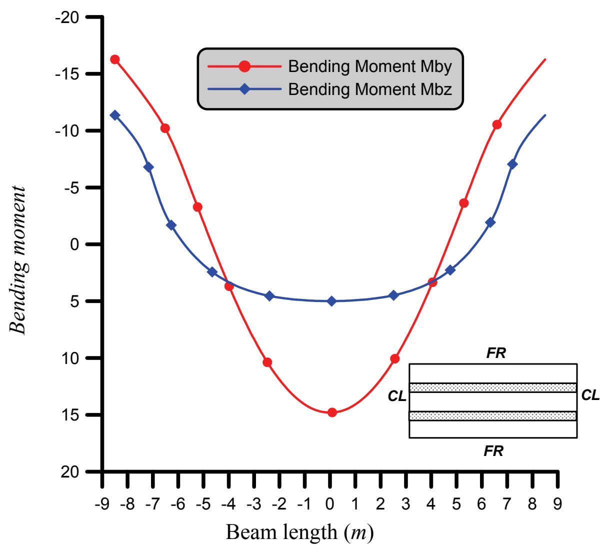

Figure 16: Bending moments M_{by}^{i} (kNm), M_{bz}^{i} (kNm) along the axis of the beams of the stiffened plate of Example 3

of which is very important in the design of prefabricated ribbed plates (estimation of bondage, shear connectors or welding).

References

Bezine, G.; Cimetiere, A.; Gelbert, J.P. (1985): Unilateral buckling of thin elastic plates by boundary integral equation method. *Int J Numerical Methods in Engineering*, vol.21, pp.2189-2199.

Botta, A. S.; Venturini, W. S. (2005): Reinforced 2d Domain Analysis Using BEM and Regularized BEM/FEM Combination, *CMES: Computer Modeling in Engineering & Sciences*, vol. 8, No. 1, pp. 15-28.

Bryan, G.H. (1891): On the stability of a plane plate under thrust in its own plane, with applications to the buckling, *Proc. London Math. Soc.*,Vol.22, pp.54–67.

Costa, J.A.; Brebbia, C.A. (1985): *Elastic buckling of plate using the boundary element method*, Boundary elements VII, Springer-Verlag, Berlin, 4/29-4/42.

Dawe, D.J. (1969): Application of the discrete element method to the buckling analysis of rectangular plates under arbitrary membrane loadings, *Aeronaut. Quart.*, vol.20, pp.114–128.

de Paiva, J.B. (1996): Boundary Element Formulation of Building Slabs, *Engineering Analysis with Boundary Elements,* vol. 17, pp. 105-110.

Divo, E; Kassab, A.J. (2005): Transient Non-linear Heat Conduction Solution by a Dual Reciprocity Boundary Element Method with an Effective Posteriori Error Estimator, *CMC: Computers, Materials & Continua*, vol.2(4), pp. 277-288.

Dziatkiewicz, G.; Fedelinski, P. (2007): Dynamic Analysis of Piezoelectric Structures by the Dual Reciprocity Boundary Element Method, *CMES: Computer Modeling in Engineering & Sciences*, vol. 17, No. 1, pp. 35-46.

Fernandes, G.R.; Venturini, W.S. (2005): Building Floor Analysis by the Boundary Element Method, *Computational Mechanics*, vol. 35, pp. 277-291.

Grondin, G.Y.; Elwi, A.E.; Cheng, J.J.R. (1999): Buckling of stiffened steel plates – a parametric study, *Journal of Constructional Steel Research*, vol.50, pp.151–175.

Hatzigeorgiou, G.D.; Beskos, D.E. (2002): Dynamic Response of 3-D Damaged Solids and Structures by BEM, *CMES: Computer Modeling in Engineering & Sciences*, vol. 3, No. 6, pp. 791-802.

Jauhorng Lin; Roger C. Duffield; Hui-Ru Shih (1999): Buckling analysis of elastic plates by boundary element method, *Engineering Analysis with Boundary Elements*, vol.23, pp.131-137.

Kakol, W. (1990). Stability Analysis of Stiffened Plates by Finite Strips, *Thin–Walled Structures*, vol.10, pp.277–297.

Kamiya, N.; Sawaki, Y.; Nakamura, Y. (1984): Postbuckling analysis by the boundary element method, *Engineering Analysis*, vol.1(1), pp.40-44.

Kapur, K.; Hartz, B. (1966): Stability of plates using the finite element method, *J. Eng. Mech. Div*, ASCE, vol.92, pp.177–195.

Katsikadelis J.T.; Sapountzakis E.J.; Zorba E.G. (1990): A BEM Approach to Static and Dynamic Analysis of Plates with Internal Supports, *Computational Mechanics*, vol.7, pp. 31-40.

Katsikadelis J.T.; Sapountzakis E.J. (1985): Torsion of Composite Bars by the Boundary Element Method, *Journal of Engineering Mechanics*, ASCE, vol.51, pp. 1197-1210.

Katsikadelis J.T.; Sapountzakis E.J. (1991): A BEM Solution to Dynamic Analysis of Plates with Variable Thickness, *Computational Mechanics*, vol.7, pp. 369-379.

Katsikadelis, J.T. (2002): *Boundary Elements*: *Theory and Applications*, Elsevier, Amsterdam-London.

Katsikadelis, J.T. (2002): The Analog Equation Method. A Boundary – only Integral Equation Method for Nonlinear Static and Dynamic Problems in General Bodies, *Theoretical and Applied Mechanics*, vol.27, pp.13-38.

Katsikadelis, J.T.; Babouskos, N. (2007): Post-buckling Analysis of Plates. A BEM based Meshless variational Solution, *Proc. 8th HSTAM International Congress on Mechanics*, Patras, Greece,12 – 14 July, I, pp.177-184.

Katsikadelis, J.T.; Kandilas, C.B. (1990): A Flexibility Matrix Solution of the Vibration Problem of Plates Based on the Boundary Element Method, *Acta Mechanica*, vol.83, pp.51-60.

Katsikadelis, J.T., (1982): *The Analysis of Plates on Elastic Foundation by the Boundary Element Method*, Thesis presented to the Polytechnic University of New York, in partial fulfillment of the requirements for the degree of Doctor of Philosophy.

Lau, S.C.W.; Hancock, G.J. (1986): Buckling of Thin Flat-Walled Structures by a Spline Finite Strip Method, *Thin–Walled Structures*, vol.4, pp.269–294.

Lie, S.T.; Yu, Guoyou; Zhao, Z. (2001): Coupling of BEM/FEM for Time Domain Structural-Acoustic Interaction Problems, *CMES: Computer Modeling in Engineering & Sciences*, vol. 2, No. 2, pp. 171-182.

Liu, C.S. (2007): Elastic Torsion Bar with Arbitrary Cross-Section Using the Fredholm Integral Equations, *CMC: Computers, Materials & Continua*, vol.5(1), pp.

31-42.

Madhujit Mukhopadhyay; Abhijit Mukherjee (1990): Finite element buckling analysis of stiffened plates, *Computers and Structures*,vol. 34, pp.795–803.

Mandolini, A.; Minutolo, V.; Ruocco, E. (2001): Coupling of Underground Pipelines and Slowly Moving Landslides by BEM Analysis, *CMES: Computer Modeling in Engineering & Sciences*, vol. 2, No. 1, pp. 39-48.

Manolis, G.D.; Beskos, D.E.; Pineros, M.F. (1986): Beam and plate stability by boundary elements. *Computers and Structures*, vol.22(6), pp.917-923.

Mansur, W. J.; Abreu, A. I.; Carrer, J. A. M. (2004): Initial Conditions Contribution in Frequency-Domain BEM Analysis, *CMES: Computer Modeling in Engineering & Sciences*, vol. 6, No. 1, pp. 31-42.

Meiwen Guo; Issam E. Harik (1992): Stability of Eccentrically Stiffened Plates, *Thin-Walled Structures*, vol.14, pp.1–20.

Miers, L. S.; Telles, J. C. F. (2004): A General Tangent Operator Procedure for Implicit Elastoplastic BEM Analysis, *CMES: Computer Modeling in Engineering & Sciences*, vol. 6, No. 5, pp. 431-440.

MSC/NASTRAN for Windows, (1999): Finite element modeling and postprocessing system. Help System Index,Version 4.0, USA.

Muller-Karger, C.M.; Gonzalez, C.; Aliabadi, M.H.; Cerrolaza, M. (2001): Three dimensional BEM and FEM stress analysis of the human tibia under pathological conditions, *CMES: Computer Modeling in Engineering & Sciences*, vol. 2, No. 1, pp. 1-14.

Nerantzaki, M.S.; Katsikadelis, J.T. (1996): Buckling of plates with variable thickness – an analog equation solution. Engineering Analysis with Boundary Elements, vol.18, pp.149-154.

Ochiai, Y. (2001): Steady Heat Conduction Analysis in Orthotropic Bodies by Triple-reciprocity BEM, *CMES: Computer Modeling in Engineering & Sciences*, vol. 2, No. 4, pp. 435-446.

Providakis, C.P. (2000): BEM / FEM Comparison Studies for the Inelastic Dynamic Analysis of Thick Plates on Elastic Foundation, *CMES: Computer Modeling in Engineering & Sciences*, vol. 1, No. 3, pp. 123-130.

Purbolaksono, J.; Aliabadi, M.H. (2005): Buckling analysis of shear deformable plates by the boundary element method, *Int J Numer Methods Eng*, vol. 62, pp.537–63.

Qinghua Qin; Yuying Huang (1990): BEM of postbuckling analysis of thin plates, *Applied Mathematical Modelling*, vol.14(10), pp.544-548.

Ramm, E.; Hofmann, T.J. (1995): *Stabtragwerke*, Der Ingenieurbau, Ed. G. Mehlhorn, Band Baustatik/Baudynamik, Ernst & Sohn, Berlin.

Rashed, Y.F. (2004): Green's First Identity Method for Boundary-Only Solution of Self-Weight in BEM Formulation for Thick Slabs, *CMC: Computers, Materials & Continua*, vol.1(4), pp. 319-326.

Sabir, A.B.; Djoudi, M.S. (1995): Elastic buckling of stiffened plates by the finite element method, *Energy Sources Tech. Conf. Exh. PD,* 70, ASME, pp.191–198.

Sanz, J.A., Solis, M.; Dominguez, J. (2006): Hypersingular BEM for Piezoelectric Solids: Formulation and Applications for Fracture Mechanics, *CMES: Computer Modeling in Engineering & Sciences*, vol. 17, No. 3, pp. 215-230.

Sapountzakis E.J.; Mokos V.G. (2007): Analysis of Plates Stiffened by Parallel Beams, *International Journal for Numerical Methods in Engineering*, vol.70, pp.1209-1240.

Sapountzakis E.J.; Katsikadelis J.T. (2000): Elastic Deformation of Ribbed Plate Systems Under Static, Transverse and Inplane Loading, *Computers and Structures*, vol.74, pp.571-581.

Sapountzakis E.J.; Mokos V.G. (2009): A Displacement Solution to Transverse Shear Loading of Composite Beams by BEM, *CMC: Computers, Materials & Continua*, vol.10(1), pp.1-39.

Sapountzakis, E.J.; Mokos, V.G. (2008): An Improved Model for the Dynamic Analysis of Plates Stiffened by Parallel Beams, *Engineering Structures,* vol.30, pp.1720-1733.

Sapountzakis, E.J.; Mokos, V.G. (2003): Warping Shear Stresses in Nonuniform Torsion by BEM, *Computational Mechanics,* vol.30(2), pp.131-142.

Sapountzakis E.J.; Mokos V.G. (2001): Nonuniform Torsion of Composite Bars by Boundary Element Method, *Journal of Engineering Mechanics*, ASCE, vol.127(9), pp. 945-953.

Sapountzakis, E.J.; Tsiatas, G.C. (2007): Flexural-Torsional Buckling and Vibration Analysis of Composite Beams, *CMC: Computers, Materials & Continua*, vol.6(2), pp. 103-116.

Seide, P. (1953). *The effect of longitudinal stiffeners located on one side of a plate on the compressive buckling stress of the plate stiffener combination*, Report No. NASA TN 2873.

Shastry, B.P.; Venkateswara Rao, G.; Reddy, M.N. (1976). Stability of stiffened plates using high precision finite elements, *Nuclear Engineering and Design*, vol.36, pp.91–95.

Sheikh, I.A.; Elwi, A.E.; Grondin, G.Y. (2003). Stiffened steel plates under combined compression and bending, *Journal of Constructional Steel Research*, vol.59, pp.911–930.

Shen Peng-Cheng; Huang Dade; Wang Zongmu (1987). Static, vibration and stability analysis of stiffened plates using B spline functions, *Computers and Structures,* vol.27, pp.73–78.

Shiah, Y.C.; Guao, T.L.; Tan, C.L. (2005): Two-Dimensional BEM Thermoelastic Analysis of Anisotropic Media with Concentrated Heat Sources, *CMES: Computer Modeling in Engineering & Sciences*, vol. 7, No. 3, pp. 321-338.

Shiah, Y.C.; Tan, C.L. (2000): Fracture Mechanics Analysis in 2-D Anisotropic Thermoelasticity Using BEM, *CMES: Computer Modeling in Engineering & Sciences*, vol.1, No. 3, pp. 91-99.

Sun, X.S.; Huang, L.X.; Liu, Y.H.; Cen, Z.Z. (2004): Elasto-plastic Analysis of Two-dimensional Orthotropic Bodies with the Boundary Element Method, *CMC: Computers, Materials & Continua*, vol.1(1), pp. 91-106.

Syngellakis, S.; Kang, M. (1987): A boundary element solution of the plate buckling problem, *Engineering Analysis*, vol.4(2), pp.75-81.

Tan, C. L.; Shiah, Y.C.; Lin, C.W. (2009): Stress Analysis of 3D Generally Anisotropic Elastic Solids Using the Boundary Element Method, *CMES: Computer Modeling in Engineering & Sciences*, vol. 41, No. 3, pp. 195-214.

Tanaka, M. (1986): *Elastic buckling analysis of assembled plate structures by boundary element method*, Boundary elements VIII, Springer-Verlag, Berlin, pp.547-559.

Timoshenko S.P. (1936): On the stability of the stiffened plates, *Der Eisenbau* (in German),vol.12, pp.147–163.

Timoshenko, S.P.; Goodier, J.N. (1951): *Theory of Elasticity*, 2^{nd} ed., McGraw-Hill Book Company, New York.

Troitsky, M.S. (1976): *Stiffened Plates, Buckling, Stability and Vibration.* Elsevier, Amsterdam.

Vörös, G.M. (2007): An improved formulation of space stiffeners, *Computers and Structures,* vol.85, pp.350–359.

Vörös, G.M. (2007): Buckling and vibration of stiffened plates, *International Review of Mechanical Engineering*, I.RE.M.E., vol.1., n.1.,pp.49–60.

Wang, P. B.; Yao, Z. H.;; Lei, T. (2006): Analysis of Solids with Numerous Microcracks Using the Fast Multipole DBEM, *CMC: Computers, Materials & Continua*, vol.3(2), pp. 65-76.

Wen, P.H., Aliabadi, M.H.; Young, A. (2006): Post buckling analysis of Reissner plates by the boundary element method, *The Journal of Strain Analysis for Engineering Design*, vol.41(3), pp.239-252.

Zhang, Ch.; Savaidis, A. (2003): 3-D Transient Dynamic Crack Analysis by a Novel Time-Domain BEM, *CMES: Computer Modeling in Engineering & Sciences*, vol. 4, No. 5, pp. 603.

Zhou, J. X.; Koziara, T.; Davies, T. G. (2006): A Fast Space-Time BEM Method for 3D Elastodynamics, *CMES: Computer Modeling in Engineering & Sciences*, vol. 16, No. 2, pp. 131-140.